Pesquisas em Geociências
GEOCIÊNCIAS
v. 52, nº 2 (2025)
doi.org/10.22456/1807-9806.147543

Research article

Rare Earth Elements in Permo-Triassic bones from the Paraná Basin, Brazil: a preliminary approach

Elementos Terras Raras em ossos Permo-Triássicos da Bacia do Paraná, Brasil: uma abordagem preliminar

Protásio A. V. Paim [1], *Leonardo Corecco* [2,3*], *Vitor P. Pereira* [4] & *Marina B. Soares* [1,5]

[1]Programa de Pós-Graduação em Geociências (PPGGEO), Instituto de Geociências, Universidade Federal do Rio Grande do Sul (UFRGS), Av. Bento Gonçalves, 9500, 91501-970, Agronomia, Porto Alegre, Rio Grande do Sul, Brasil. protasio.paim@ufrgs.br.
[2]Universidade Federal de Pelotas, Unidades e Cursos de Graduação, Centro de Engenharias (CENG). Engenharia Geológica, Campus Alfândega, Praça Domingos Rodrigues, n° 2, Porto, CEP - 96010450, Pelotas, RS, Brasil. leonardo.corecco@ufpel.edu.br.
[3]Programa de Pós-graduação em Diversidade Biológica e Recursos Naturais, Universidade Regional do Cariri, Crato-CE, Brasil.
[4]Departamento de Mineralogia e Petrografia, Instituto de Geociências, Universidade Federal do Rio Grande do Sul (UFRGS), Av. Bento Gonçalves, 9500, 91501-970, Agronomia, Porto Alegre, Rio Grande do Sul, Brasil. vitor.pereira@ufrgs.br.
[5]Departamento de Geologia e Paleontologia, Museu Nacional, Universidade Federal do Rio de Janeiro (UFRJ), Av. Bartolomeu de Gusmão, 875, São Cristovão, 20941-160, Rio de Janeiro, RJ, Brazil. marina.soares@mn.ufrj.br.

Abstract: Rare-earth elements, yttrium and fluorine contents were analyzed in fifteen fossil bones and their bearing rocks. These samples came from Permian (Irati and Rio do Rasto formations) and Triassic (Santa Maria Supersequence) sedimentary layers of Paraná Basin, Brazil. Analyzes were performed using ICP-MS for REE and selective electrode for fluorine. All bone samples have much higher REE contents than their respective sedimentary host rocks. Statistical correlations indicated that F is the main complexing agent of REE and Y in these fossil bones. After comparing the REE signatures of the sedimentary rocks with those from the bones contained in them, it was possible to verify that they represent peripheral assemblages. The Ce anomalies allowed the differentiation of reducing environments from oxidizing ones, and the LREE/HREE ratios indicated the degree of acidity of these environments. The Y/Ho ratios made it possible to identify, in the case of the Irati Formation (early Permian), the contribution of continental sediments to the marine environment. These findings corroborate previous faciological/paleoenvironmental studies that were carried out on the same localities where the studied fossils were collected. In addition to that, the analytical results showed significant variations within the distribution patterns of REE and Y in fossils and their sedimentary host rocks, and their distribution patterns are not related to a specific taxonomic group.

Keywords: ICP-MS analyses; Irati Formation; Rio do Rasto Formation; Santa Maria Supersequence.

Recebido: 05/2025
Aceito: 08/2025
Publicado: 09/2025

Resumo: Elementos terras raras, ítrio e flúor foram analisados em quinze ossos fósseis e suas rochas hospedeiras. Essas amostras provêm de camadas sedimentares do Permiano (formações Irati e Rio do Rasto) e do Triássico (Supersequência Santa Maria) da Bacia do Paraná, Brasil. Análises foram conduzidas utilizando-se ICP-MS para os ETR e eletrodo seletivo para flúor. Todos as amostras de ossos possuem teores muito mais elevados de ETR do que suas respectivas rochas sedimentares. Correlações estatísticas indicaram que F é o principal agente complexante de ETR e Y nesses ossos fósseis. Após comparar as assinaturas de ETR das rochas sedimentares com aqueles dos ossos nelas preservados, foi possível verificar que estes representam assembleias periféricas. As anomalias de Ce permitiram diferenciar os ambientes redutores dos oxidantes, já as razões ETRL/ETRP indicaram o grau de acidez desses ambientes. As razões Y/Ho tornaram possível identificar, no caso da Formação Irati (Permiano inicial), a contribuição de sedimentos continentais para o ambiente marinho. Esses achados corroboraram com os estudos faciológicos/paleoambientais conduzidos anteriormente nas mesmas localidades nas quais os fósseis estudados foram coletados. Além disso, os resultados analíticos mostraram variações significativas dentro do padrão de distribuição de ETR e Y tanto nos fósseis quanto nas rochas sedimentares que os preservaram, e seus padrões de distribuição não estão relacionados a grupos taxonômicos específicos.

Palavras-chave: Análises por ICP-MS; Formação Irati; Formação Rio do Rasto; Supersequência Santa Maria.

1. Introdução

Bioapatite is the main component of vertebrate bones. It is comprised of an inorganic (mineral) fraction formed by hydroxylapatite [Ca5(PO4)3(OH)] that usually contains carbonate in its structure and organic components, especially collagen (Newesely, 1989; Wopenka & Pasteris, 2005; Pasteris *et al.*, 2008). In general, bone apatite contains about 7 wt.% carbonate and tooth enamel around 3.5 wt.% (Daculsi *et al.*, 1997; Elliott, 2002; Wopenka & Pasteris, 2005).

The fossilization begins with the necrological processes that encompass the death and the organisms' decomposition (necrolysis). Right away, the organic remains are subject to the action of biostratinomic processes (e.g., disarticulation, transport, reworking, burial). By the end, there are the diagenetic processes that, in this scenario, are named fossildiagenetic (Simões *et al.*, 2010). Generally, during the biostratinomic phases, there is a predominance of biological and physical processes (e.g., trampling, necrophagy, water transport), whereas in the fossildiagenetic phase, most are physical-chemical and geological (e.g., tectonics, sedimentation; Simões *et al.*, 2010; Araújo-Júnior & Bissaro-Júnior, 2017; Zabini *et al.*, 2017).

At this point, there is collagen degradation, and gradually bones can be preserved by replacing organic molecules with mineral particles, which occurs by recrystallization and permineralization of bioapatite by chemical elements transported by water (Daculsi *et al.*, 1997; Elliott, 2002; Wopenka & Pateris, 2005). As collagen is lost, simultaneous structural rearrangement of the remaining inorganic matrix (for the crystallinity increases) used to occur. There is also evidence for the spatial redistribution of bone mineral because of microbial attack (e.g., Turner-Walker & Syverson, 2002), which can affect porosity at the intermediate and perhaps coarse (macro-) scales (Hedges, 2002), affecting REE uptake in the bones.

During the bone's diagenesis, trace elements (e.g., Fe, Sr, Mn, Mg, rare earth elements and yttrium) can be incorporated into the bones replacing the calcium site within the hydroxylapatite structure (Wopenka & Pasteris, 2005; Trueman *et al.* 2008a) or crystallize secondary minerals in the cavities. These elements are weakly bonded to chemical complexes of the water percolating the bones. The process is modulated by environmental factors, such as fluid pH, redox conditions, concentrations of elements in fluids, geochemical activity, and colloidal reactions (Erel & Stolper, 1993; Johannesson & Zhou, 1997; Dia *et al.*, 2000; Johannesson *et al.*, 2000; Gruau *et al.*, 2004).

The REE and Y contents in fresh bones are commonly low, measured by either ppb or ppt levels (Kohn *et al.*, 1999; Herwartz *et al.*, 2011), whereas in fossil bones, they can reach high orders of magnitude (hundreds to thousands of ppm). The incorporation of REE in bones likely occurs during the early stages of fossildiagenesis, before 100.000 years (Trueman & Tuross, 2002; Kohn, 2008; Trueman *et al.* 2008a; Koenig *et al.*, 2009; Suarez *et al.*, 2010). Therefore, REE and Y contents in fossil bones are directly related to the depositional context shortly after the organism's death. So, bones from different stratigraphic units and/or geographic locations may have different REE distribution patterns (Staron *et al.*, 2001; Patrick *et al.*, 2004; Martin *et al.*, 2005; Trueman *et al.*, 2005). This information is valuable to several subjects, such as taphonomy and provenance (geographic and stratigraphic positioning) studies (Trueman *et al.*, 2008a, 2008b; MacFadden *et al.*, 2012; Suarez *et al.*, 2007; Suarez *et al.*, 2010; Tütken *et al.*, 2011); paleo-redox evaluations (Elderfield & Pagett, 1986; German & Elderfield, 1990; Grandjean-Lécuyer *et al.*, 1993); forensic investigations and the identification of smuggled material (Lukens *et al.*, 2009; Suarez, 2004; Suarez *et al.*, 2009; Terry Jr. *et al.*, 2009); paleoenvironmental reconstructions (Metzger *et al.*, 2004; Patrick *et al.*, 2004; Martin *et al.*, 2005; Anderson *et al.*, 2007); paleoceanographic investigations (Elderfield & Pagett, 1986; Wright *et al.*, 1987; Martin & Scher, 2004), and evaluations of the contemporaneity (time averaging) between faunistic elements of fossil assemblages (Purdy *et al.*, 2015).

Herein, we conducted a comparative evaluation on REE content in fossil bones from several tetrapod groups from Permo-Triassic geological units of the Paraná Basin, Southern Brazil, as well as in their sedimentary host rocks, aiming to verify the REE patterns. In addition, we sought geochemical signatures that could distinguish fossils from different localities and stratigraphic contexts for provenance studies. Finally, we aimed to determine whether there is any characteristic REE distribution among the sampled taxonomic groups.

2. Geological and Stratigraphic Context

The intracratonic Paraná Basin is localized in the central-eastern part of the South American plate, encompassing portions of Brazil, Paraguay, Argentina, and Uruguay. This basin has approximately 1.7 million km^2 (Fig. 1) and is up to 7.000 m thick at its deepest portions (Schneider *et al.*, 1974; Holz *et al.*, 2010). The Paraná Basin has nearly 400 Myr of geological history, from Ordovician to Cretaceous (Milani *et al.*, 2007). It is divided into six second-order stratigraphic supersequences (Milani *et al.*, 1998), from the base to the top: Rio Ivaí (Ordovician-Silurian), Paraná (Devonian), Gondwana I (Carboniferous-Early Triassic), Gondwana II (Middle-Late Triassic), Gondwana III (Late Jurassic-Early Cretaceous), and Bauru (Late Cretaceous). The first three sequences are sedimentary successions of transgressive-regressive cycles associated with sea level oscillations during Paleozoic (Milani *et al.*, 2007). The other three (Fig. 1) are composed of continental sedimentary packages associated with igneous rocks (Milani *et al.*, 2007).

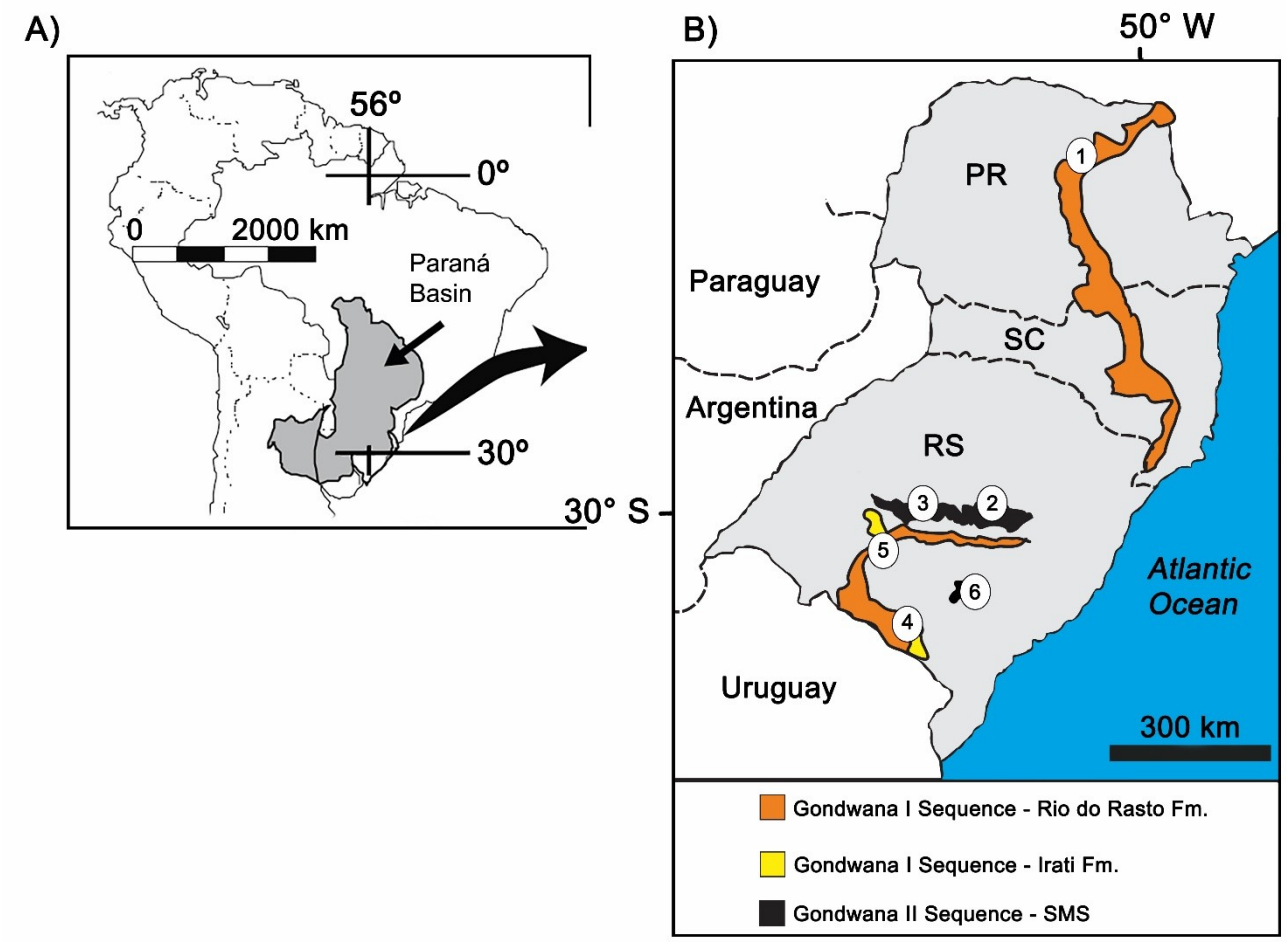

Figure 1. A) Location map of the Paraná Basin in South America with detail of outcropping areas of Gondwana I and Santa Maria supersequences in Southern Brazil. B) Simplified stratigraphic chart of the Paraná Basin (modified after Milani *et al.*, 2007). SMS = Santa Maria Supersequence; Fm. = Formation; PR = Paraná State; SC = Santa Catarina State; RS = Rio Grande do Sul State. Numbers 1 to 6 indicate the approximate location of fossil sites which the studied bones came from. 1 = Ortigueira and São Jerônimo da Serra; 2 = Candelária, Porto Mariante, Santa Cruz do Sul and Venâncio Aires; 3 = Agudo and Dona Francisca; 4 = Bagé and Aceguá; 5. São Gabriel; 6 = Santana da Boa Vista.

Figura 1. A) Mapa de localização da Bacia do Paraná na América do Sul com detalhe para as áreas aflorantes de Gondwana I e Supersequência Santa Maria no Sul do Brasil. B) Carta estratigráfica simplificada da Bacia do Paraná (modificada após Milani et al., 2007). SMS = Santa Maria Supersequence; Fm. = Formação; PR = Estado do Paraná; SC = Estado de Santa Catarina; RS = Estado do Rio Grande do Sul. Números de 1 a 6 indicam a localização aproximada dos sítios fossilíferos de onde os ossos estudados provêm. 1 = Ortigueira e São Jerônimo da Serra; 2 = Candelária, Porto Mariante, Santa Cruz do Sul e Venâncio Aires; 3 = Agudo e Dona Francisca; 4 = Bagé e Aceguá; 5. São Gabriel; 6 = Santana da Boa Vista.

This research was carried out on the fossil bones of tetrapods from sedimentary units belonging to Gondwana I (Irati and Rio do Rasto formations; Fig. 2) and Gondwana II (Santa Maria Supersequence; Fig. 2).

The Gondwana I Supersequence has the highest sedimentary volume of the Paraná Basin, representing a complete transgressive-regressive cycle (Milani *et al.*, 1998). The Irati (IF) and Rio do Rasto (RRF) formations represent, respectively, the maximum flooding of the cycle and the establishment of continental depositional systems (delta lobes, lacustrine pellites, and aeolian sandstones) that silted up the remaining basin.

The Gondwana II Supersequence comprises the Middle-Late Triassic continental packages from South Brazil (Milani *et al.*, 1998). It stratigraphically corresponds to Santa

Maria and Caturrita formations (sensu Andreis *et al.*, 1980) and Mata Sandstone (sensu Zerfass *et al.*, 2003). Zerfass *et al.* (2003) renamed this supersequence as Santa Maria (SMS), subdividing it into three third-order sequences (from base to the top): Santa Maria I, Santa Maria II, and Santa Maria III. Horn *et al.* (2014) distinguished a new sequence between Santa Maria I and II, reorganizing and renaming the package as Pinheiros-Chiniquá (= Santa Maria I), Santa Cruz (new sequence), Candelária (= Santa Maria II), and Mata (= Santa Maria III) (Fig. 2).

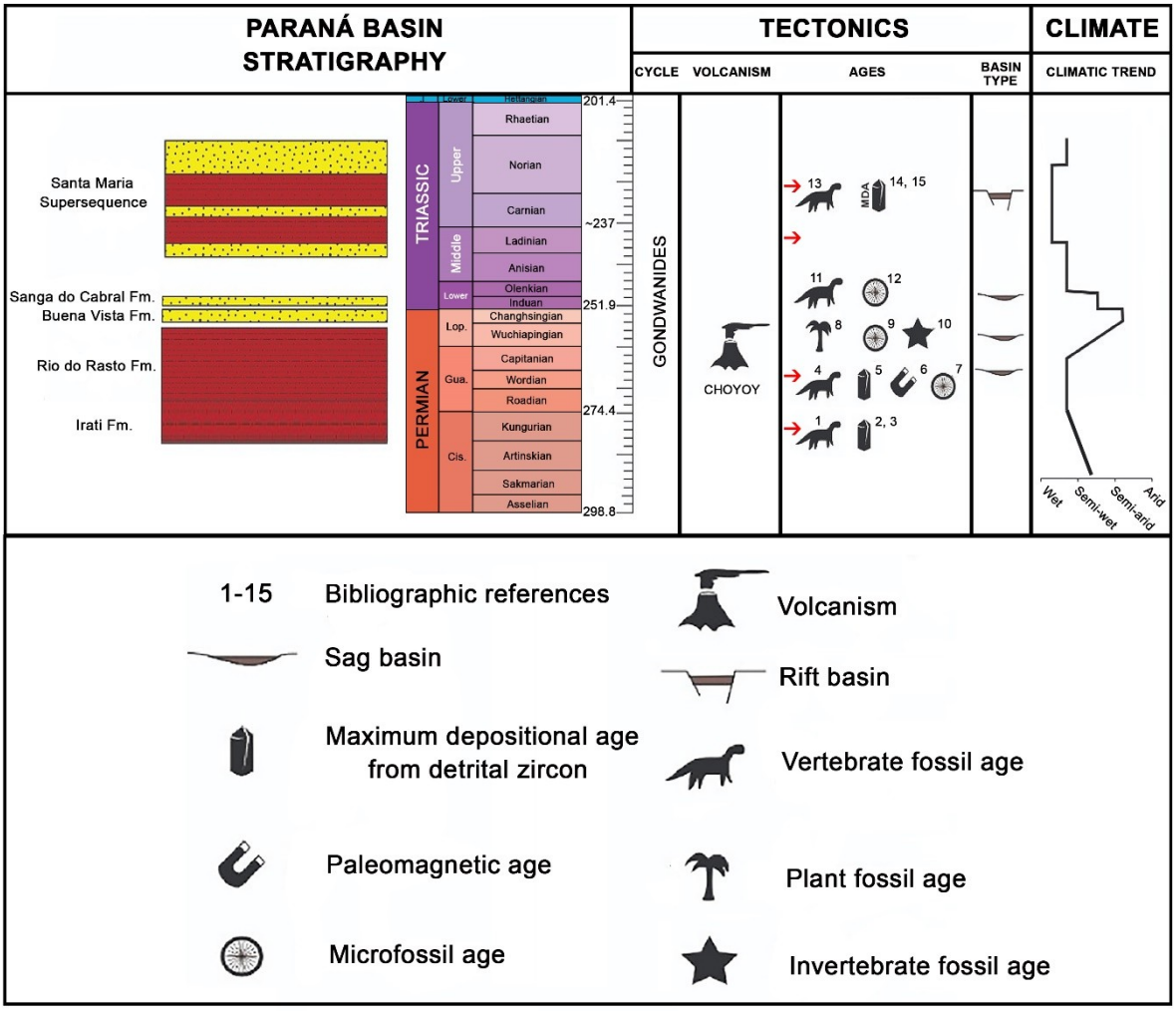

Figure 2. Stratigraphic-tectonic-climatic-geochronologic integrated evolution for Paraná Basin. The figure compiles data from Scherer *et al.* (2023) and presents the bibliography used to constrain the unit ages. Unit age constraints from 1 - Adami Rodrigues *et al.* (2016); 2 - Santos *et al.* (2006); 3 - Philipp *et al.* (2023); 4 - Francischini *et al.* (2018); 5 - Francischini *et al.* (2018); 6 - Ernesto *et al.* (2020); 7 - Rohn & Rösler (1990); 8 - Rohn & Rösler (2000); 9 - Neregato (2007); 10- Langer *et al.* (2009); 11 - Dias-da-Silva *et al.* (2017); 12 - Schultz *et al.* (2020); 13 - Schultz *et al.* (2020); 14 - Philipp *et al.* (2018); 15 - Langer *et al.* (2018). Red arrows indicate the studied units. Ages in Paraná Basin Stratigraphy section are from Cohen *et al.* (2024). J = Jurassic.

Figura 2. Evoluções estratigráfica-tectônica-climática-geocronológica integradas para a Bacia do Paraná. A figura compila dados de Scherer et al. (2023) e apresenta a bibliografia utilizada para restringir as idades das unidades. 1 - Adami Rodrigues et al. (2016); 2 - Santos et al. (2006); 3 - Philipp et al. (2023); 4 - Francischini et al. (2018); 5 - Francischini et al. (2018); 6 - Ernesto et al. (2020); 7 - Rohn & Rösler (1990); 8 - Rohn & Rösler (2000); 9 - Neregato (2007); 10- Langer et al. (2009); 11 - Dias-da-Silva et al. (2017); 12 - Schultz et al. (2020); 13 - Schultz et al. (2020); 14 - Philipp et al. (2018); 15 - Langer et al. (2018). Setas vermelhas indicam as unidades estudadas. As idades na seção estratigráfica da Bacia do Paraná vêm de Cohen et al. (2024). J = Jurássico.

The Irati Formation (Gondwana I) was dated as Late Artinskian (278.4 ± 2.2 Myr), based on SHRIMP-U/Pb zircons from bentonitic layers (Santos *et al.*, 2006). Recent 238U/206Pb dating performed on detrital zircons from volcanic ash layers suggest a maximum depositional age of 273.2 ± 7 Myr for the Irati Formation (Philipp *et al.*, 2023). This unit is placed at the base of the Passa Dois Group, and subdivided it into two members, Taquaral (lower) and Assistência (upper), which together are 40 m thick (Milani *et al.* 2007). The depositional environment of the Irati Formation corresponds to a vast epicontinental deoxidized to anoxic water shallow sea (named Whitehil Irati Sea) whose connection with the open ocean was widened during the Assistência Member deposition time. This epicontinental sea corresponds to the area where today is the southern Brazil (Irati Formation), Paraguay, Uruguay (Mangrullo Formation), southeastern Namibia and South Africa (Whitehill Formation, Nama and Karoo Basins; Lavina, 1991; Xavier *et al.*, 2018). The environmental conditions of Irati Formation were characterized by an alternating dry-humid seasonal climate with variating water salinity (Araújo, 2001; Holz *et al.*, 2010; Goldberg & Humayun, 2016). A diverse fossil fauna has been recovered from the Assistência Member, such as: mesosaurids (Mesosaurus tenuidens, Stereosternum tumidum and Brazilosaurus sanpauloensis), paleonisciformes fishes, Pygocephalomorpha crustaceans, ostracods, foraminifera, brachiopods, and sponges (Oelofsen & Araujo 1983; Adami-Rodrigues *et al.* 2016).

The Rio do Rasto Formation is located at the upper portion of the Passa Dois group and represents a subsidence phase followed by a definitive continentalization of the deposition systems of the Paraná Basin (Milani *et al.*, 2007). It is subdivided into two members, the Serrinha (upper) and Morro Pelado (lower) members (Schneider *et al.*, 1974; Ng *et al.*, 2019). The Morro Pelado Member, which contains the fossils studied in this research, is mainly composed of finely granulated, tabulate, lenticular, or laminated sandstone, as well as red claystones (Rohn, 1994; Holz *et al.*, 2010; Francischini *et al.*, 2018). It corresponds to the most arid phase recorded on Rio do Rasto Formation, which is characterized by coalescent alluvial-fan deposits with a wide floodplain subjected to flooding and formation of shallow river channels associated with aeolian sediments (Rohn *et al.*, 2005; Schemiko *et al.*, 2014). This unit bears a wide variety of fossils such as palynomorphs (Neregato *et al.*, 2008), root marks (Azevedo *et al.*, 2018), ostracods, conchostracan, mollusks (Simões *et al.*, 2015; Guerrini *et al.*, 2020), hybodontiformes sharks (Pauliv *et al.*, 2017) actinopterygian fishes (Richter & Langer, 1998; Malabarba *et al.*, 2003), temnospondyli amphibians (Barberena & Dias, 1998; Dias & Barberena, 2001), pareiasaurids (Araújo, 1985), basal anomodonts, dicynodonts, and dinocephalians (Langer, 2000; Cisneros *et al.*, 2011, 2012; Boos *et al.*, 2013, 2016). Affinities between the terrestrial tetrapod faunas of the Morro Pelado Member with others from Africa and Russia indicate a Guadalupian/Lopingian age (Boos *et al.*, 2015; Fig. 2). One outcrop of the Morro Pelado Member of Rio Grande do Sul state, located in Aceguá municipality (Fig. 1B), was dated by Francischini *et al.* (2018) by SHRIMP based on U–Pb isotopic contents of zircons. Results indicated a 270.61 +1.76/-3.27 Myr age (early Guadalupian).

The establishment of the Santa Maria Supersequence (Middle to Late Triassic, Gondwana II) was controlled by tectonic events that formed the South Brazil rifting associated with the Gondwanides Orogeny (Milani *et al.*, 2007; Zerfass *et al.*, 2003).

The sequences of the Santa Maria Supersequence were dated, from the base to the top, as follows: 241 Myr (Ladinian; Pinheiros-Chiniquá Sequence; Dinodontosaurus AZ; Philipp *et al.*, 2023), 237 ± 1.5 Myr (Early Carnian; Santa Cruz Sequence; Santacruzodon AZ; Philipp *et al.*, 2018), 233.23 ± 0.73 Myr (Late Carnian; base of Candelária Sequence; Hyperodapedon AZ; Langer *et al.*, 2018) and 225.42 ± 0.37 Myr (Early Norian; top of

Candelária Sequence; Riograndia AZ; Langer *et al.*, 2018). All these data were obtained from U-Pb analyses of detrital zircons, which means that they represent the maximum depositional age of these units.

The Pinheiros-Chiniquá sequence is composed by red layers of massive and laminated siltstone and mudstone with sparse lenses of fine-grained sandstone, interpreted as fluvial deposits that later changed to shallow lacustrine deposits (Zerfass *et al.*, 2003). The Santa Cruz Sequence (Santacruzodon AZ) encompasses red mudstones resembling that of the Pinheiros-Chiniquá Sequence, but interbedded with sandstones and conglomerates. The deposition of Pinheiros-Chiniquá and Santa Cruz sequences occurred under arid/semi-arid conditions, resulting in the formation of carbonate concretions and calcretes (Zerfass *et al.*, 2003; Horn *et al.*, 2013). Horn *et al.* (2018a) described these deposits as dry loess mudflats (aeolian dust) with an occasional reworking by ephemeral streams. Despite that, rhizoliths and early diagenetic features (e.g., micrite crusts) recently reported for the Santacruzodon AZ (Schoenstatt Sanctuary site; Santa Cruz Sequence) indicate several pedogenically modified levels (calcic vertisols). These features can be linked to the Carnian Pluvial Episode (CPE), but its reported age of 236.6 ± 1.5 Ma either bears reevaluation or potentially extends the duration of the CPE (Battista & Schultz, 2022; Battista *et al.*, 2024a). These sequences are marked by abundant kannemeyeriiform dicynodont fossils such as Stahleckeria potens and especially Dinodontosaurus sp., associated with cynodonts (e.g., Traversodon stahleckeri, Massetognathus ochagaviae, Bonacynodon schultzi, Aleodon cromptoni, and the traversodontids Santacruzodon hopsoni, Menadon besairiei and Massetognathus ochagaviae; Melo *et al.*, 2015; Martinelli *et al.*, 2016, 2017; Schmitt *et al.*, 2019). The Stenaulorhynchinae rhynchosaur Brasinorhynchus mariantensis, proterochampsids (e.g., Proterochampsa nodosa, Pinheirochampsa rodriguesi) and “rauisuchians” (non-Crocodylomorpha loricatans) such as Prestosuchus chiniquensis and Dagasuchus santacruzensis, and Hyperodapedontinae rhynchosaur remains were also recovered within these AZs (Huene, 1942; Price, 1947; Lacerda *et al.*, 2015; Schultz *et al.*, 2016; Battista *et al.*, 2024b; Paes-Neto *et al.*, 2024).

The Candelária Sequence demarcates an increasing humidity phase in the Santa Maria Supersequence (Scherer *et al.*, 1995; Corecco *et al.*, 2020). At its base (Hyperodapedon AZ), Candelária Sequence is comprised of medium- to fine-grained, cross-bedded sandstones and mudstones lenses, arranged by thick mudstones in its middle portion (Zerfass *et al.*, 2003). At the top, there is a coarsening succession of siltstones and mudstones intercalated with lenses of fine cross-bedded sandstones and massive sandstones facies (channel fill deposits; Zerfass *et al.*, 2003; Horn *et al.*, 2018b). This last portion is a result of an ephemeral fluvial system with catastrophic floods generated by severe seasonal precipitation with high sedimentary load (Horn *et al.*, 2018b). These assemblage zones (Hyperodapedon AZ and Riograndia AZ) comprise a massive presence of the rhynchosaur Hyperodapedon sp., followed by abundant records of the Traversodontidae cynodont Exaeretodon riograndensis (Schultz, 2005; Abdala *et al.*, 2002); probainognathian cynodonts with different corporal sizes (e.g., Prozostrodon brasiliensis, Trucidocynodon riograndensis, Brasilodon quadrangularis, Riograndia guaibensis; Bonaparte & Barberena, 2001; Martinelli *et al.*, 2005; Oliveira *et al.*, 2010; Soares *et al.*, 2011); lagerpetids (e.g. Ixalerpeton polesinensis, Venetoraptor gassenae, Faxinalipterus minimus; Kellner *et al.*, 2022; Müller *et al.*, 2023), and some of the some of the oldest dinosaurs ever described (e.g., Staurikosaurus pricei, Saturnalia tupiniquim, Macrocollum itaquii; Langer *et al.*, 1999; Cabreira *et al.*, 2011, 2016; Müller *et al.*, 2018), some of the oldest dinosaurs ever described. For more information about the Santa Maria Supersequence fauna, see Schultz *et al.* (2020) review.

3. Brief taphonomic aspects

The mesosaurid bones from the Irati Formation of Rio Grande do Sul state evaluated in this study were preserved in carbonate tempestitic layers (Soares, 2003). This multi-episodic event was the result of mass mortality and may have been generated by severe storms and/or by a bottom bioclastic input and subsequent storm reworking (Xavier *et al.*, 2018). The specimens preserved under these conditions are often found in varying degrees of disarticulation, ranging from partially articulated skeletons to isolated and abraded bone fragments (Soares, 2003).

The Permian continental tetrapods studied in this research came from two outcrops of the Rio do Rasto Formation (Morro Pelado Member) located in the states of Paraná and Rio Grande do Sul. These depositional environments were characterized as distal alluvial fans connected with fluvial plains (Rohn *et al.*, 2005). A taphonomic model where a continental shallow aquatic environment, with sporadic water supply, was proposed by Azevedo *et al.* (2018) as the conditioning of these fossils' preservation. As a result, for the sporadic floods, an attritional deposition of carcasses, with several articulation degrees (from semi-articulated post-cranial remains to isolated skulls and lower jaws), was established.

The Santa Maria Supersequence fossils (Middle-Late Triassic) also have several types of disarticulations, including complete skeletons, semi-articulated remains and totally isolated bones (Holz & Souto-Ribeiro, 2000). Pronounced alternating dry and humid seasons, marked by intense floods, characterized the climate of Rio Grande do Sul state during this time (Scherer & Faccini, 1994, Holz & Souto-Ribeiro, 2000). According to Scherer & Faccini (1994), during the flood seasons, most of the alluvial plains kept submerged forming a series of shallow lacustrine bodies. The cyclic floods were responsible for the death of animals and for reworking the bones of previously dead animals (attritional death). These bones were then disarticulated, and their remains were scattered through the floodplain regions (Holz & Souto-Ribeiro, 2000). Subsequently, they were exposed to subaerial conditions during the dry season with the lowering of the phreatic level. Besides that, some carcasses of animals killed by the flooding might have been transported over long distances as "inflated carcasses" before being deposited and buried.

The taphocoenoses of the Irati and Rio do Rasto formations and the Santa Maria Supersequence are composed by bones of animals that could have died at different times (time averaging). Some of these bones could have been transported prior to the fossilization, and even after their burial, they might have suffered reworking and transportation again. If the geochemical conditions of the sedimentary layers that preserved these fossils were different, this would have been chemically recorded in the bones. So, that is why the distribution pattern and content of REE, Y and other elements (especially trace elements), have been used as an excellent criterion to test autochthony and recognize bones from different strata (Trueman, 2008).

4. Institutional abbreviations

UFRGS-PV- Universidade Federal do Rio Grande do Sul, Museu de Paleontologia Irajá Damiani Pinto/Paleovertebrate Collection, Porto Alegre, Rio Grande do Sul, Brazil; MMACR-PV-T - Museu Municipal Aristides Carlos Rodrigues, Paleovertebrate Triassic Collection, Candelária, Rio Grande do Sul, Brazil; UFPR-PV - Universidade Federal do Paraná, Curitiba, Paraná, Brazil.

5. Materials and analytical methods

A total of 15 samples of fossil bones fragments (three mesosaurids, two temnospondyls' amphibians, one pareiasaurid, two dicynodonts, three cynodonts, two rhynchosaurs, one "rauisuchian", and one undetermined archosaur) and its surrounding sedimentary rocks were selected (Chart 1).

5.1 Sample's preparation

The samples were extracted and prepared with chisels, tips and other pertinent materials, looking to reduce the fossil damage (Feldmann, 1989; Silva Santos, 1998). The tools were sanitized between sample disaggregation with 70% alcohol to minimize contamination. Purity control was performed using a binocular stereoscopic microscope and histological needles to separate the bone fragments. In this process, cortical bone fragments were preferably separated for analysis. To diminish possible contamination, even millimeter and submillimeter-sized bone fragments were removed from the different sedimentary rock samples. The samples were then macerated with the aid of a mortar and pestle to the clay size (≤ 0.064 mm) to optimize the analytical results. These procedures were carried out at the Paleovertebrate Laboratory of the Universidade Federal do Rio Grande do Sul.

5.2 ICP-MS and fluorine analyses

The REE and Y analyses were performed by ICP-MS and F with the specific electrode at the ACME Labs in Canada. The respective REEs lower and upper detection limits (ppm) were the following: La (0.1 and 50,000); Ce (0.1 and 50,000); Pr (0.02 and 10,000); Nd (0.3 and 10,000); Sm (0.05 and 10,000); Eu (0.02 and 10,000); Gd (0.05 and 10,000); Tb (0.01 and 10,000); Dy (0.05 and 10,000); Ho (0.02 and 10,000); Er (0.03 and 10,000); Tm (0.01 and 10,000); Yb (0.05 and 10,000); Lu (0.01 and 10,000); Y (0.1 and 50,000); and F (10 and 10,000).

5.3 Sample normalizations

Normalization of REEs by standards is a necessary procedure to compare their contents and distribution patterns in different samples. This procedure is used because elements with even atomic numbers are more abundant than those with odd atomic numbers, generating a zig-zag pattern in the distribution diagrams (Oddo-Harkins Effect). In this study, the REE contents of fossil bones and sedimentary rocks were normalized by the C1 chondrite (Anders & Grevesse, 1989), North American Shale Composite (NASC; Haskin & Frey, 1966; Haskin & Haskin, 1966; Haskin *et al.*, 1968), and post-Archean Australian Shale (PAAS) (Taylor & McLennan, 1985). Normalization by C1 chondrite showed the best results for our samples because it eliminated the zig-zag pattern, which did not occur with normalization against PAAS. As many of the REEs were not analyzed by NASC, this standard was not used.

REE, Y and F in the different samples of bones and sedimentary rocks were compared considering their contents and distribution patterns: (1) The relationships among the contents of REE, Y and F; (2) REE and Y distribution pattern in rock samples; (3) REE and Y distribution pattern in bones; (4) Relationship between REE and Y content of bones and their bearing rocks; (5) REE and Y distribution within fossils of a same taxonomic group, and (6) REE and Y distribution patterns of bones by their originating rocks (without normalization) in each geological unit. Although Y has an ionic radius and geochemical behavior similar to those of the HREE (see Shannon, 1976), in this work, it was placed on the graphs after Lu to facilitate comparison with the behavior of the other REE.

Chart 1. Description and provenience of the sampling used for geochemical analyses by ICP-MS. T.I. = Taxonomic identification; SED. = Sedimentary rocks; AZ = Assemblage Zone; n.a. = not applicable; RS = Rio Grande do Sul State; PR = Paraná State. Triassic samples – O1A, S1A to O4B, S4B; Permian samples – O5A, S5A to O7A, S7A. The red dashed line indicates the limit between the Permian and Triassic samples.

Quadro 1. Descrição e proveniência das amostras utilizadas para as análises geoquímicas por ICP-MS. T.I. = Identificação taxonômica; SED. = Rochas sedimentares; AZ = Zonas de Associação; n.a. = Não se aplica; RS = Estado do Rio Grande do Sul; PR = Estado do Paraná. Amostras do Triássico – O1A, S1A a O4B, S4B; Amostras do Permiano – O5A, S5A a O7A, S7A. A linha tracejada vermelha indica o limite entre as amostras do Permiano e do Triássico.

SAMPLE	T.I.	BONE	UNIT	AZ	AGE	SED.	LOCALITY	CATALOG Nº
O1A, S1A	Rauisuchia *Prestosuchus*	Rib	Pinheiros-Chiniquá	*Dinodontosaurus*	Late Ladinian	Clayey siltite; Pelite	Dona Francisca, RS	UFRGS-PV-0629-T
O1B, S1B	Dicynodontia *Dinodontosaurus*	Vertebra					Mariante, RS	UFRGS-PV-0300-T
O2A, S2A	Cynodontia *Menadon*	Lower jaw	Santa Cruz	*Santacruzodon*	Early Carnian	Clayey siltite; Pelite	Santa Cruz do Sul, RS	UFRGS-PV-1165-T
O2B, S2B	Cynodontia Undetermined	Skull					Venâncio Aires, RS	UFRGS-PV-0457-T
O3A, S3A	Cynodontia *Exaeretodon*	Lower jaw	Candelária (base)	*Hyperodapedon*	Late Carnian	Clayey siltite; Pelite	Agudo, RS	UFRGS-PV-1226-T
O3B, S3B	Rhynchosauria *Hyperodapedon*	Rib					Vale do Sol, RS	UFRGS-PV-1206-T
O3C, S3C	Rhynchosauria *Hyperodapedon*	Skull					Santana da Boa Vista, RS	UFRGS-PV-1248-T
O4A, S4A	Dicynodontia *Jachaleria*	Rib	Candelária (top)	*Riograndia*	Early Norian	Clayey siltite; Pelite	Candelária, RS	UFRGS-PV-0540-T
O4B, S4B	Archosauria Undetermined	Limb bones					Candelária, RS	MMACR-PV-012-T
O5A, S5A	Mesosauridae	Rib	Irati	n.a.	Cisuralian	Marl	São Gabriel, RS	UFRGS-PV-0272-P
O5B, S5B	Mesosauridae	Vertebra					Aceguá, RS	UFRGS-PV-0607-P
O5C, S5C	Mesosauridae	Rib					São Gabriel, RS	UFRGS-PV-0597-P
O6A, S6A	Temnospondyli Undetermined	Skull fragments	Rio do Rasto	n.a.	Guadalupian	Clayey siltite; Pelite	São Jerônimo da Serra, PR	UFPR-0150-PV
O6B, S6B	Temnospondyli *Australerpeton*	Limb bones					Ortigueira, PR	UFRGS-PV-0320-P
O7A, S7A	Pareiasauria *Provelosaurus*	Limb bones					Bagé, RS	UFRGS-PV-0231-P

6. Results

6.1 ICP-MS analyses

The ICP-MS results of the analyses of the fossil bones and their respective sedimentary rocks are in the Supplementary Material Table S1.

Based on ICP-MS analyses, ΣREE, ΣLREE, ΣHREE, ΣLREE/ΣHREE, and Y/Ho ratios were calculated. Furthermore, to understand the geochemical mobility and fixation of REE in bones during the fossilization processes, bone enrichment factors were calculated. Enrichment in bones was calculated by dividing the REE content in the bones by that in the sedimentary rocks that contained them. All results are presented in Table 2.

Table 2. Summary of the ΣREE, ΣLREE, ΣHREE, ΣLREE/ΣHREE, Y/Ho, and REE enrichment factors. O = Fossil bones samples; S = Sedimentary rock samples; B/R = Bone content/ Sedimentary Matrix content ratio. The red dashed line indicates the limit between the fossil bones and the sedimentary rocks samples.

Tabela 2. Resumo dos ΣREE, ΣLREE, ΣHREE, ΣLREE/ΣHREE, Y/Ho e fator de enriquecimento dos ETR. O = Amostras de ossos fósseis, S = Amostras de rochas sedimentares; B/R = Razão do Conteúdo registrado no osso/Conteúdo registrado na matriz sedimentar. A linha tracejada vermelha indica o limite entre as amostras de ossos fósseis e de rochas sedimentares.

Samples	ΣREE	ΣLREE	ΣHREE	ΣLREE/ΣHREE	Y/Ho
O1A	3,485.72	3,180.60	305.12	10.424	32.56
O1B	2,033.82	1,825.99	207.83	8.786	33.22
O2A	6,932.17	6,046.98	885.19	6.831	30.95
O2B	10,308.05	8,776.52	1,531.53	5.731	34.60
O3A	10,247.25	9,247.91	999.34	9.254	34.47
O3B	8,668.02	7,784.90	883.12	8.815	33.10
O3C	976.04	866.71	109.33	7.927	31.31
O4A	9,203.65	8,038.74	1,164.91	6.901	29.27
O4B	7,669.65	6,666.69	1,002.96	6.647	29.44
O5A	5,111.07	4,658.69	452.38	10.298	38.00
O5B	17,155.71	15,663.30	1,492.41	10.495	30.18
O5C	4,702.82	4,222.01	480.81	8.781	34.51
O6A	4,661.30	4,113.41	547.89	7.508	24.79
O6B	7,337.49	6,316.77	1,020.72	6.189	26.54
O7A	7,910.41	5,530.91	2,379.50	2.324	34.85
S1A	105.95	91.70	14.25	6.435	29.31
S1B	312.34	280.00	32.34	8.658	34.36
S2A	415.71	373.87	41.84	8.936	46.22
S2B	129.55	111.60	17.95	6.217	31.40
S3A	166.60	147.99	18.61	7.952	30.74
S3B	236.66	212.49	24.17	8.791	29.05
S3C	255.89	227.81	28.08	8.113	28.78
S4A	5,375.04	4652.89	722.15	6.443	26.59
S4B	410.00	352.55	57.45	6.137	30.35
S5A	25.09	20.37	4.72	4.316	35.77
S5B	3,069.07	2,684.42	384.65	6.979	34.06
S5C	129.75	116.69	13.06	8.935	39.88
S6A	258.51	228.79	29.72	7.698	24.39
S6B	137.16	118.37	18.79	6.300	27.77
S7A	207.02	169.81	37.21	4.564	30.48

Samples	B/R Enrichment Factors		
	ΣREE	ΣLREE	ΣHREE
1A	32.90	34.68	21.41
1B	06.51	06.52	06.43
2A	16.68	16.17	21.16
2B	79.57	78.64	85.32
3A	61.51	62.49	53.70
3B	36.63	36.64	36.54
3C	03.81	03.80	03.89
4A	01.71	01.73	01.61
4B	18.71	18.91	17.46
5A	203.71	228.70	95.84
5B	05.59	05.83	03.88
5C	36.25	36.18	36.82
6A	18.03	17.98	18.44
6B	53.50	53.36	54.32
7A	38.21	32.57	63.95

Based on these results, it was possible to establish the following considerations about the sedimentary rocks and the fossils hosted on them.

6.2 REE, Y, and F content relationships

Regarding F levels, it is possible to verify that in sedimentary rocks, their values are always lower than 10,000 ppm. This tenor is the limit of detection of F by the selective electrode. In several bone analyses (O2B, O3B, O4A, O4B, O5A, O5B, O5C, O6B, and O7A), the F values exceeded the detection limit, preventing their use for correlations. Therefore, these samples were excluded from the F correlations.

The relationships among the REE, F, and Y concentrations in bones and rocks are displayed in Figure 3.

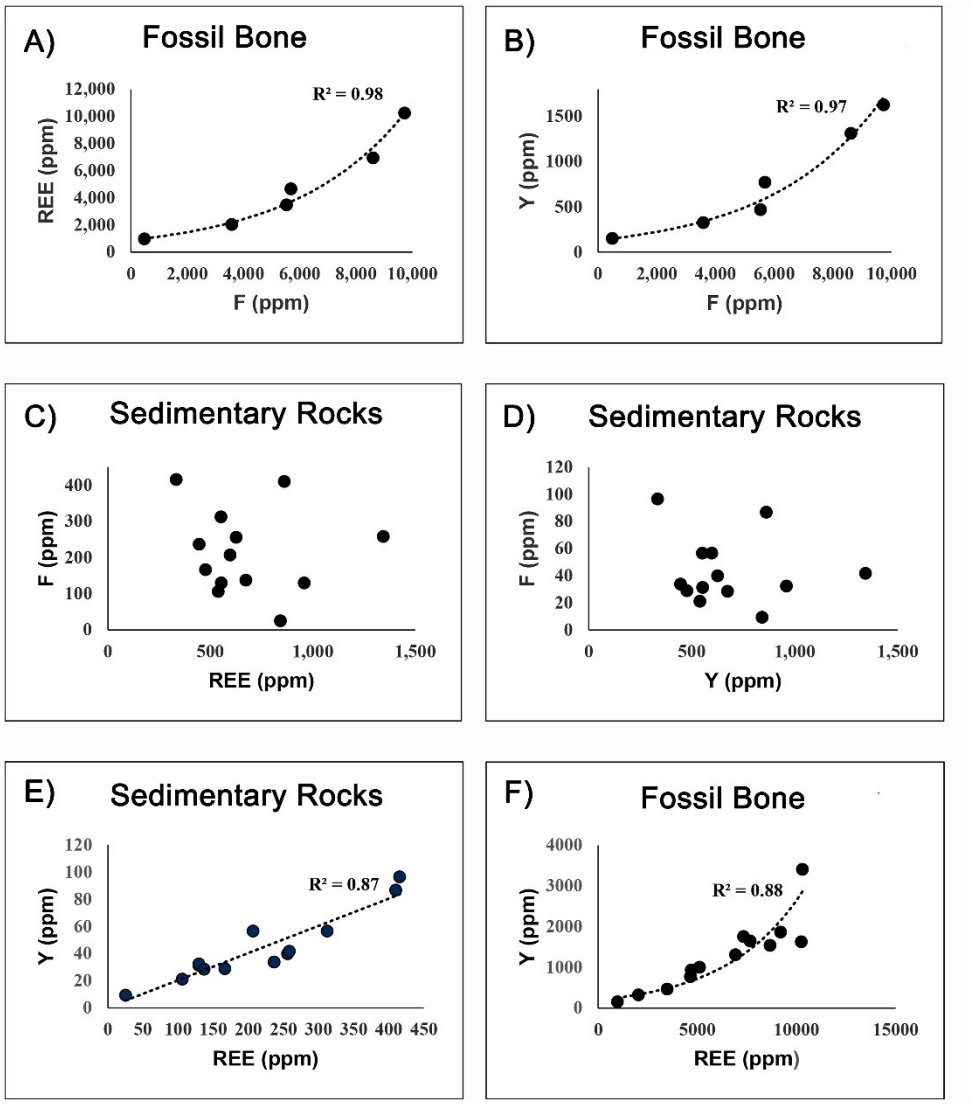

Figure 3. A) Presents an exponential correlation between the F contents and REE in fossil bones. B) Shows an exponential correlation between the F contents and Y in fossil bones. C) Presents an absence of correlation between the REE contents and F in sedimentary rocks. D) Shows an absence of correlation between the Y contents and F in sedimentary rock. E) and F) present a correlation between REE and Y in sedimentary rocks and fossil bones.

Figura 3. A). Apresenta uma correlação exponencial entre os conteúdos de F e ETR nos ossos fósseis. B) Mostra uma correlação exponencial entre os conteúdos de F e Y nos ossos fósseis. C) Apresenta uma ausência de correlação entre os conteúdos de ETR e F nas rochas sedimentares. D) Mostra uma ausência de correlação entre os conteúdos de F e Y nas rochas sedimentares. E) e F) apresentam uma correlação entre ETR e Y nas rochas sedimentares e ossos fósseis.

It is possible to see the exponential increase in REE and Y contents with the rise of F contents in the fossil bones studied (Figs. 4A and 4B). However, there are no correlations between REE or Y with F in the sedimentary host rocks (Figs. 4C and 4D). Nevertheless, Y correlates positively with REE in sedimentary rocks and exponentially in fossil bones (Figs. 4E and 4F). Furthermore, there was an increasing exponential correlation between the F and REE content in bones from different geological unities ($R^2 = 0.98$; Fig. 3A), and between the F and Y content in these bone samples ($R^2 = 0.97$; Fig. 3B). The samples S4A and S5B (Figs. 3C and 3D) were excluded because they have relatively high contents of REE and Y and, if they are plotted on the graph, they would force a false positive correlation.

When plotting LREE vs. Y and HREE vs. Y in sedimentary rocks, it is seen that there is a high linear correlation in both cases (R2 = 0.86). However, for bones, HREE exhibits a linear correlation ($R^2 = 0.95$), and for LREE ($R^2 = 0.74$), even after excluding samples O5B and O7A, which have anomalous Y and LREE concentrations. This correlation is smaller ($R^2 = 0.68$) if the regression is exponential. It means that Y behaves like an HREE when incorporated into bones.

The enrichment factors (O/S; Tab. 2) for the REE are always positive. It confirms that bones are enriched in REE when compared with their sedimentary host rocks. Significant differences occur in all stratigraphic units, depending on local geochemical conditions. In most bone samples, the LREE and HREE enrichment factors are similar. Samples 2A, 2B, and 7A have higher HREE contents, while in 1A, 3A, and 5A, the LREE are higher. This is due to local biogeochemical factors responsible for the complexation, transport, and precipitation of REE.

6.3 REE and Y distribution pattern in sedimentary rock samples

The distribution of REE and Y of sedimentary rocks normalized by C1 chondrite is shown in Figure 4.

In all sedimentary rock samples, the LREE contents are higher than the HREE. Furthermore, the HREE distribution patterns are relatively horizontal, independent of the ΣREE. This indicates that geochemical environmental changes interfere less with these elements than with LREE.

The Ce anomalies varied among sedimentary rocks from different geological units and among samples from the same stratigraphic level. The increase of Ce in some stratigraphic units is due to their oxidation (Ce^{3+} to Ce^{4+}). Ce^{4+} is geochemically less mobile and is precipitated in sedimentary rocks (Braun *et al.*, 1990).

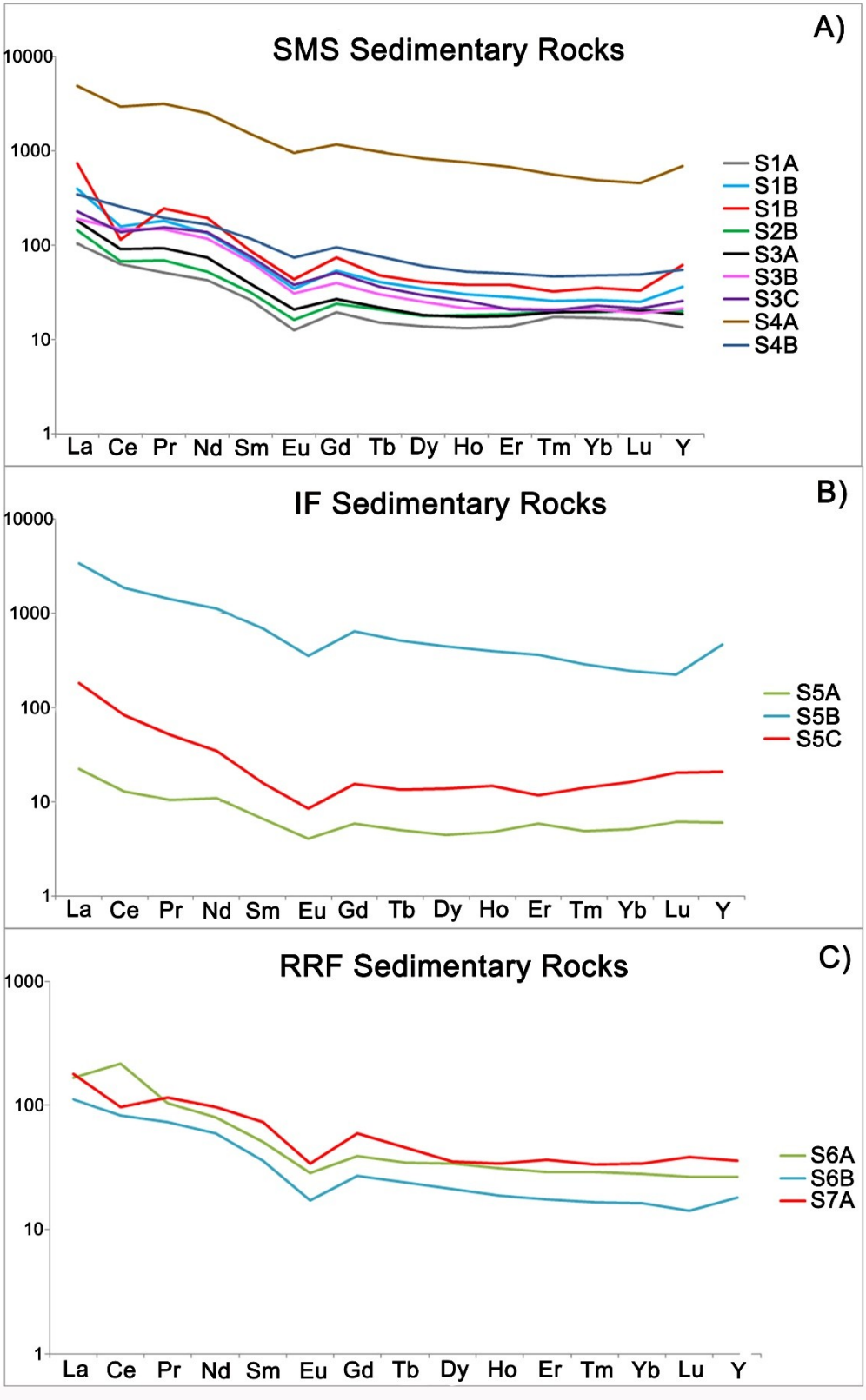

Figure 4. Distribution of REE and Y normalized by the C1 chondrite of sedimentary rock samples. A) Santa Maria Supersequence; B) Irati Formation; C) Rio do Rasto Formation. Abbreviations: SMS = Santa Maria Supersequence; IF = Irati Formation; RRF = Rio do Rasto Formation.

Figura 4. Distribuição de ETR e Y normalizados pelo condrito C1 nas amostras de rochas sedimentares. A) Supersequência Santa Maria; B) Formação Irati; C) Formação Rio do Rasto. Abreviações: SMS = Supersequência Santa Maria; IF = Formação Irati; RRF = Formação Rio do Rasto.

6.4 REE and Y distribution pattern in fossil bones

The distribution of REE and Y contents of fossil bones normalized by C1 chondrite is shown in Figure 5.

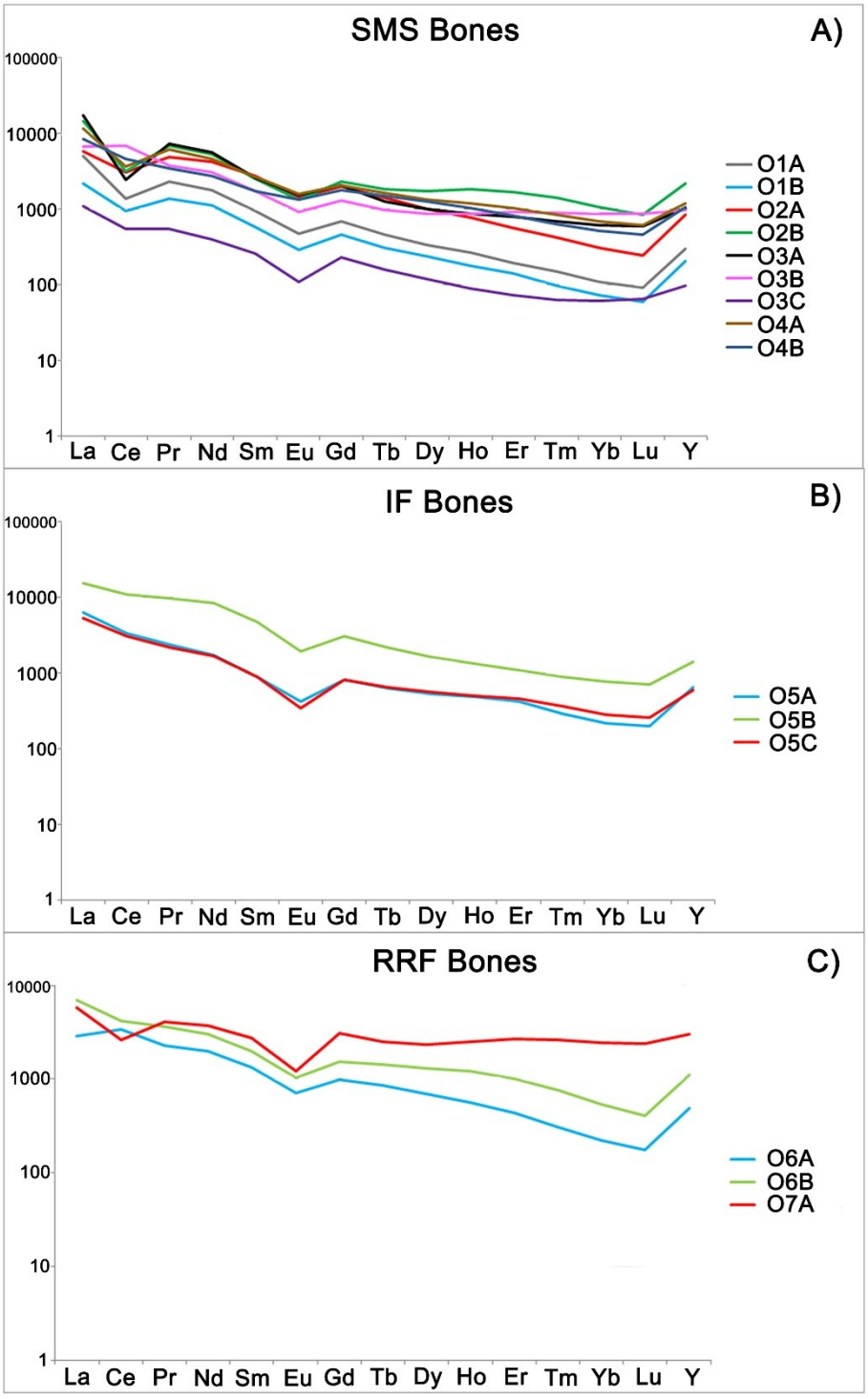

Figure 5. Distribution of REE and Y in fossil bones from the different geological units studied, despite their taxonomic classification. A) Santa Maria Supersequence; B) Irati Formation; C) Rio do Rasto Formation. Abbreviations: SMS = Santa Maria Supersequence; IF = Irati Formation; RRF = Rio do Rasto Formation.

Figura 5. Distribuição de ETR e Y nos ossos fósseis das diferentes unidades geológicas estudadas, apesar de sua classificação taxonômica. A) Supersequência Santa Maria; B) Formação Irati; C) Formação Rio do Rasto. Abreviações: SMS = Supersequência Santa Maria; IF = Formação Irati; RRF = Formação Rio do Rasto.

The REE contents of fossil bones are always much higher than those of the rocks that contain them. The distribution patterns of these elements are similar to those of these rocks, and some particularities are described below.

Comparing the REE and Y distribution patterns of fossil bone samples from the Santa Maria Supersequence, it is possible to highlight that all samples are enriched in LREE, but the total REE contents are different. Some differences are also observed in HREE, where samples O3B and O3C have more horizontal distribution patterns. The only sample with a positive Ce anomaly is O3B, so this anomaly indicates that this sample was exposed to oxidizing conditions, at least at the moment when it incorporated the REE. The small negative Ce anomaly in sample O4B indicates that the fossilization environment was not as reduced as the others, which is also registered by the reduction in the negative Eu anomaly. Concerning Y, it appears that sample O3B also differs from the others in that it has a much lower content in this element, confirming that the oxidizing environment also interfered with the HREE distribution pattern (Fig. 5A).

All REE signatures of the Irati Formation are similar, but the sample O5B, which came from another locality, is enriched in the total content of these elements. The small negative Ce anomalies in all samples indicate that fossilization environments are slightly reducing during the REE incorporation. The samples S5A and S5C are from the same locality, and their HREE distribution patterns are slightly horizontal. The fossil samples O5A and O5C are enriched in HREE, but their distribution patterns decrease with increasing atomic numbers. It means that adsorption and/or diadochic Ca substitutions were greater for the elements with an ionic radius closer to that of Ca. In addition to that, in these samples, the Y content increases more than in the O5B sample. These differences in distribution patterns should be due to the geochemical differences in carbonate environments during the fossilization processes (Fig. 5B).

At the Rio do Rasto Formation, the HREE patterns of samples O6A and O6B, from Paraná state, were similar. However, sample O6A exhibited a positive Ce anomaly, and sample O6B showed a slightly negative Ce anomaly, indicating variations in oxidation conditions among these distinct localities. The O7A sample, from Rio Grande do Sul state, has an accentuated negative Ce anomaly, and its REE distribution pattern is very different from those of the Paraná state samples. Resembling IF, the fossil samples O6A and O6B are enriched in HREE, and their distribution patterns decrease with increasing atomic numbers for the reasons explained above (Fig. 5C).

The geochemical behavior of Y in sedimentary rocks is different from that in the bones contained within them. This means that fossilization processes have interfered significantly in the distribution patterns of the REE, especially HREE, but some characteristics, such as Ce and Eu anomalies, are preserved.

6.5 REE and Y distribution within fossils of the same taxonomic group

The distribution pattern of REE and Y in bones from each taxonomic group, regardless of their sedimentary context, is displayed in Figure 6.

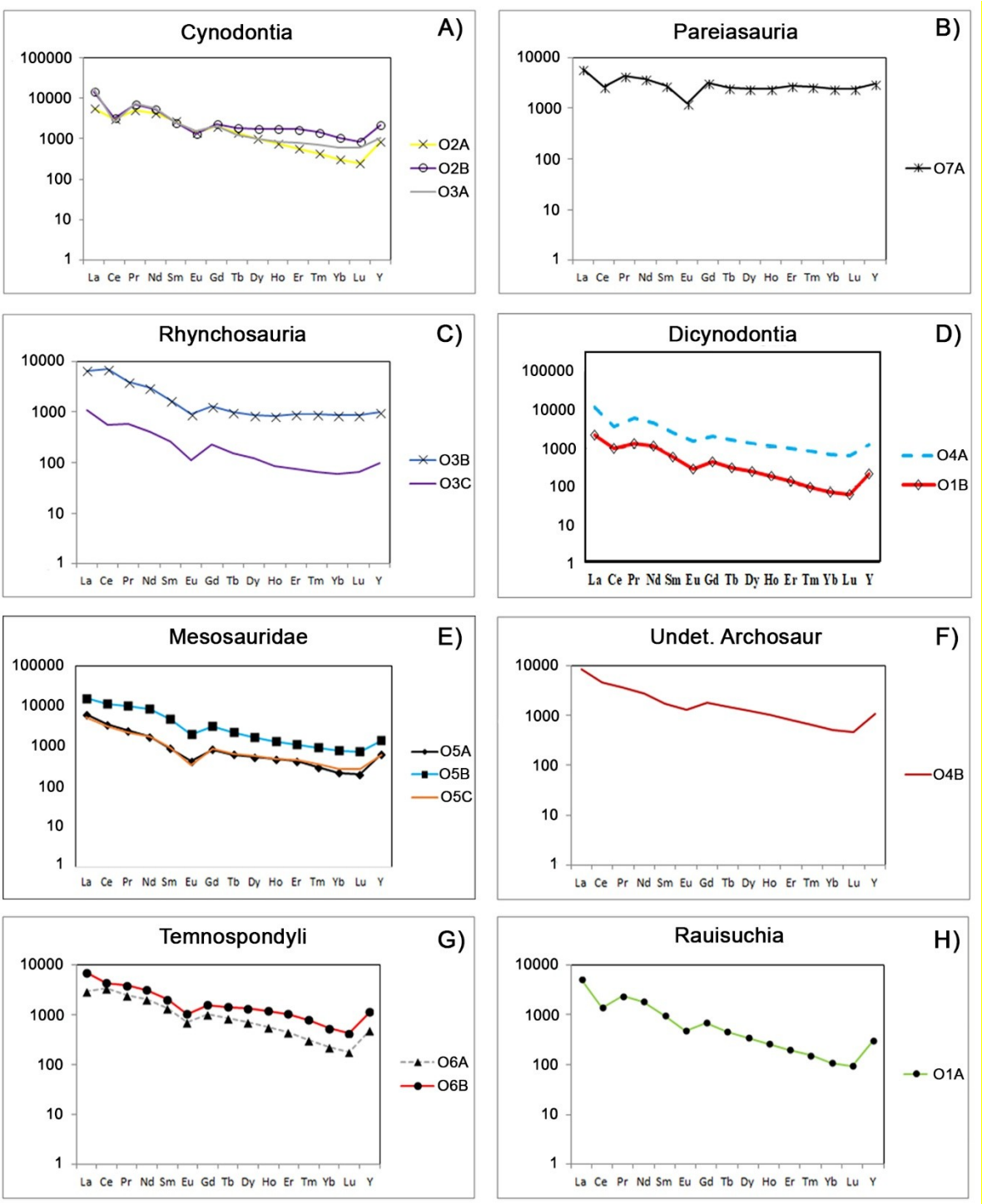

Figure 6. REE and Y distribution in the fossil bones from the same taxonomic group apart of their sedimentary context.

Figura 6. Distribuição de ETR e Y nos ossos fósseis do mesmo grupo taxonômico, independentemente de seu contexto sedimentar.

The studied Cynodontia samples (Fig. 6A) have great similarity in the contents and distribution of the LREE. However, the HREE concentration and distributions are significantly different. The HREE values from the sample O2A decrease much more with the increase of the atomic number, and the O2B presents the highest HREE values. All samples have negative anomalies of Ce and Eu.

The sample O7A (Fig. 6B) has a distribution pattern of the REEs almost horizontal if the negative anomalies of Ce and Eu are not considered. The REE signature of this sample is very different from those of the Temnospondyli amphibians (samples O6A and O6B) from the Rio do Rasto Formation registering the different geochemical conditions of fossilization.

Two rhynchosaurs bones (samples O3B and O3C) were compared (Fig. 6C). The sample O3B, from Vale do Sol municipality, has a positive Ce anomaly, and the sample O3C, from Santana da Boa Vista municipality, has a negative Ce anomaly. The different ΣREE values and HREE distribution patterns of these samples suggest that the fossilization processes in these locations were significantly different.

The samples of Dicynodontia (O1B from the Pinheiros-Chiniquá Sequence and O4A from the top of the Candelária Sequence) have almost identical REE distribution patterns (Fig. 6D). The O4A sample has higher REE content, but the HREE distribution in the O1B sample decreases more with the increase of the atomic number. A common feature in the distribution patterns of dicynodont bones here is the negative Ce and Eu anomaly.

The REE distribution patterns are almost identical in all three Mesosauridae samples (O5A, O5B, and O5C) (Fig. 6E). The sample O5B, from the municipality of Aceguá, has the highest ΣREE, probably due to the high content of bone fragments in the sedimentary rock matrix that does not change the distribution pattern of these elements. All samples have negative anomaly of Eu and very small one of Ce. The identical signatures of the samples O5A and O5C are due to their origin from the same locality.

The sample O4B (Fig. 6F) belongs to an undetermined archosaur and exhibits an incipient negative anomaly in Ce and a more pronounced anomaly in Eu. Comparing the samples O4B and O4A, which are derived from the same stratigraphic level and the same municipality, it is possible to note that O4B has a distinct REE distribution pattern and lower LREE and HREE contents when compared to O4A. This confirms that different geochemical conditions (that are related to the REE signatures) can exist within the same locality.

The REE distribution pattern is similar in all Temnospondyli amphibians' samples (Fig. 6G) from the Rio do Rasto Formation. The sample O6A has a positive Ce anomaly, unlike the O6B, whose anomaly is negative and has the highest total REE content. This difference also records the existence of very different fossilization conditions in this formation.

The sample O1A from the Pinheiros-Chiniquá Sequence (Fig. 6H) belongs to the Rauisuchia and exhibits strong negative Ce and Eu anomalies. The REE distribution pattern is slightly different from that of the other fossil samples, as there is a marked depletion of HREE with the increase in atomic number.

Regarding SMS fossil bones, it can be concluded that only the O3B sample was exposed to oxidation. All IF fossils exhibit a small negative Ce anomaly, indicating that they have fossilized in reducing environments. The fossil samples from RRF exhibit totally different REE signatures, and only sample O6A displays a positive Ce anomaly. The sample S6A also exhibits a positive Ce anomaly, indicating that both the rock and the bone within it have been exposed to oxidation, at least in the initial stages of their fossil diagenesis.

The LREE/HREE comparison of the studied fossils made it possible to conclude that all faced acid conditions at least at the beginning of their fossildiagenesis.

Regarding Y content, only samples O3B and O7A do not show a positive anomaly. It is also verified that Y has a similar geochemical behavior to HREE. The positive Y/Ho ratios of all samples indicate that the environments studied were alkaline.

6.6 Relationship between REE and Y content of bones with that of their host rocks

The linear correlation (R) and the coefficients of determination (R^2) made it possible to compare the behavior of the REE + Y of sedimentary rocks with that of the fossil bones contained therein (Fig. 7). Therefore, R means that when the content of an element increases in the rock its concentration in the corresponding fossil bone also increases, maintaining the distribution pattern. R^2 indicates the dispersion among the analyzed points.

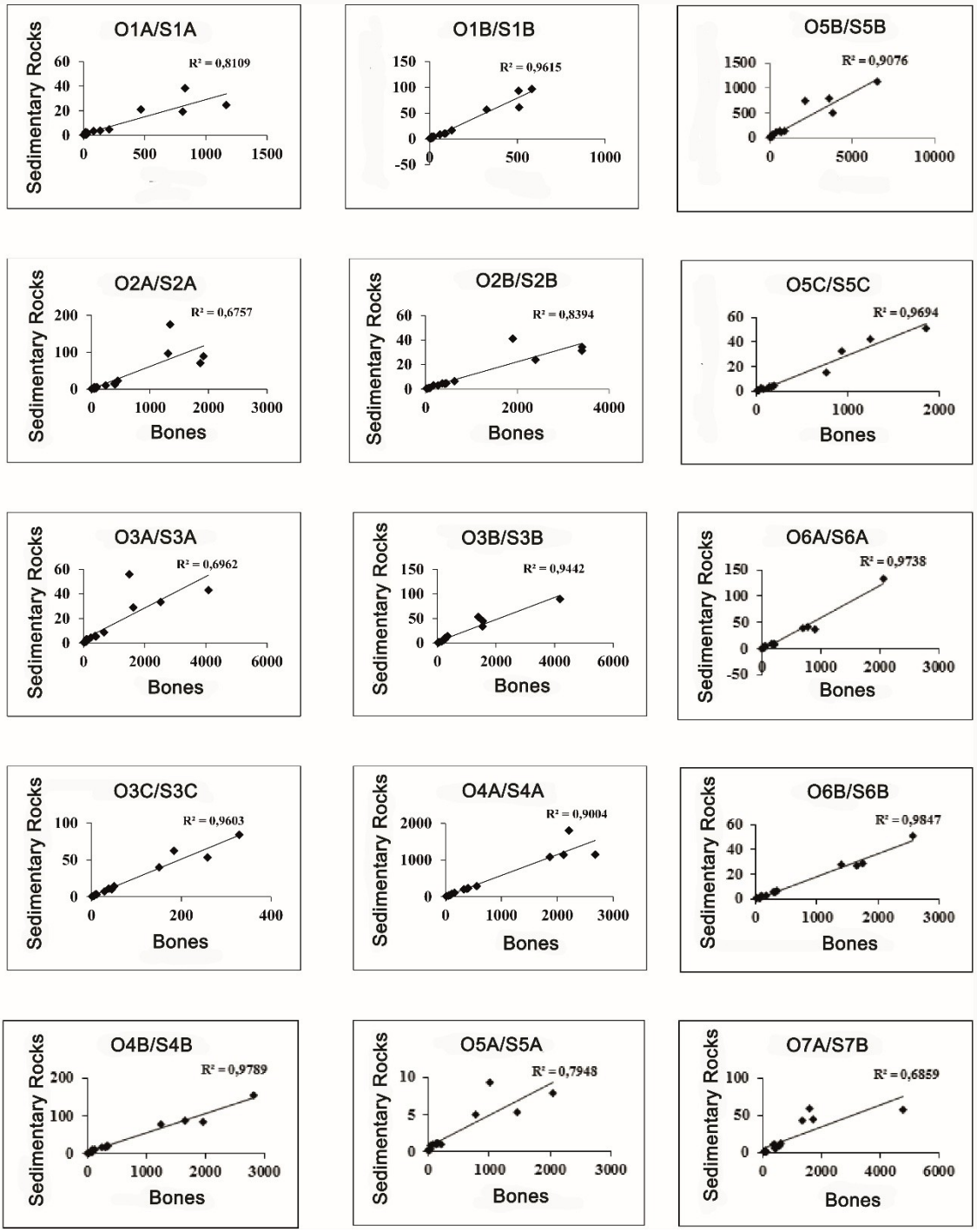

Figure 7. Relationship between the REE + Y contents in the fossil bones with those from their respective sedimentary rocks.

Figura 7. Relação entre os conteúdos de ETR + Y nos ossos fósseis com os de suas respectivas rochas sedimentares.

It can be seen from all the graphs in Fig. 7 that there is a significant correlation between the REE contents of the bones and those of the sedimentary rocks that host them. This proves that fossil bones accurately record levels of elements inherited from the sedimentary rocks that preserved them. However, when observing the dispersion coefficients, it appears that the samples with R^2 values lower than 0.80 (2A, 3A, 5A, and 7A) have only one element with a distribution point far from the straight line, often La or Ce. This discrepancy always occurred on the ordinate axis, which corresponds to the sedimentary rocks' elements. Thus, the La and Ce would only be distributed along the straight line if their contents were much higher in bones. It means that in bones, these elements were not proportionally incorporated from their matrices. Local physicochemical factors must have been responsible for the reduced incorporation. Besides that, when all the samples are considered as a set, there was no relationship between the Ce contents in sedimentary rocks and the positive or negative anomalies of this element. This indicates that the Ce incorporation in fossil bones is not only related to oxidation or reduction (Ce^{3+} or Ce^{4+}). Furthermore, the Y concentrations, such as that of sample 5A, also contributed to the lack of correlation between the tenors found in fossil bones (high contents) with those in the respective sedimentary rocks (low contents). When this element was removed, the correlations increased markedly.

It is important to highlight that many bone samples with high negative or positive Ce anomaly have high R^2. For instance, sample 3B (rhynchosaur) has a positive Ce anomaly (Fig. 7) and a high R^2 (0.94). It means that the distribution and correlation coefficients are not related to the anomaly, but rather because they measure the relationship between the contents of the elements in the bones and those in the respective sediments.

6.7 REE + Y distribution patterns resulting from the normalization of fossil bones by their sedimentary rock matrices (O/S)

The REE and Y distribution patterns originated from the fossil bones' normalizations by their sedimentary rock matrices are displayed in Figure 8. This normalization allowed us to observe the enrichment or depletion of REE and Y contents of the bones in relation to their host rocks. Additionally, the ordinate axis is not on a logarithmic scale.

Watching the O/S relationship from the studied stratigraphic units makes it possible to verify that they are extremely variable due to the great geochemical differences within the studied places. In relation to SMS, samples 2B, 3A, and 1A present the highest enrichment factor due to the relatively high LREE contents (see Tab. 2). Furthermore, these samples are the only ones that have negative Ce anomalies and relatively high Y contents. The O/S factor is lower in the samples 2A and 3B, which are enriched in this element and have a positive Ce anomaly. Sample 3B is the only one that is enriched in HREE. The other SMS samples have flat O/S distribution patterns with relatively small REE enrichment. Although significant differences are found in the contents of some elements in different SMS samples, the comparative graph of the O/S values of LREE with those of HREE in these samples shows extremely similar distribution patterns. This is because when the LREE contents increase in a sample, the HREE values also increase.

Regarding the Irati Formation (IF), the three samples have completely different O/S factors, and only sample 5A has its factor extremely high. This is due to the relatively large enrichment in LREE, including Ce which has a small positive anomaly. In Fig. 8 it is also seen that the samples 5A and 5C have negative Eu anomaly.

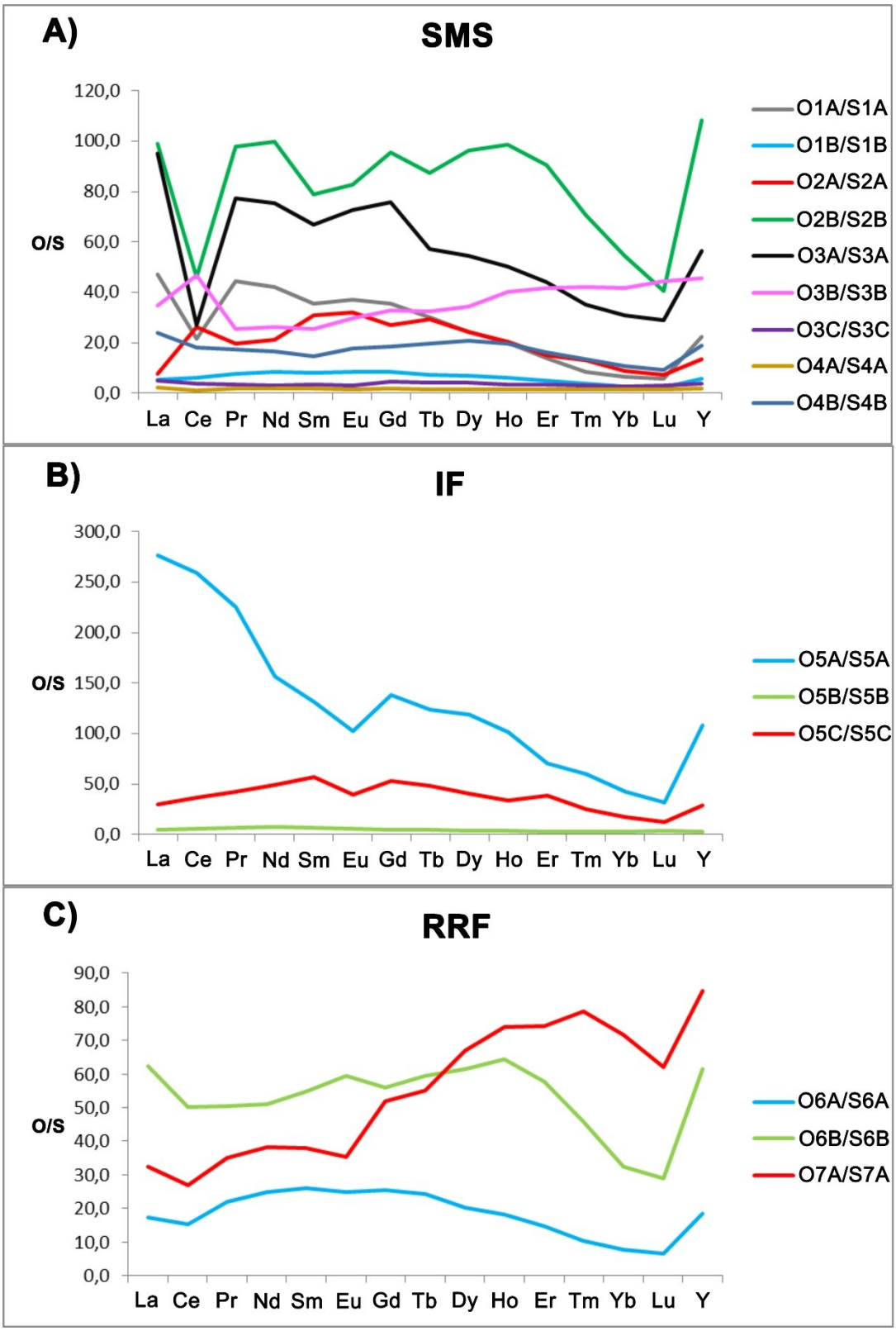

Figure 8. Distribution patterns resulting from the normalization of the fossil bones by their sedimentary rocks matrices (O/S) for each unit. A) Santa Maria Supersequence; B) Irati Formation; C) Rio do Rasto Formation. Abbreviations: SMS = Santa Maria Supersequence; IF = Irati Formation; RRF = Rio do Rasto Formation.

Figura 8. Padrões de distribuição resultantes da normalização dos ossos fósseis por suas matrizes rochosas sedimentares (O/S) para cada unidade. A) Supersequência Santa Maria; B) Formação Irati; C) Formação Rio do Rasto. Abreviações: SMS = Supersequência Santa Maria; IF = Formação Irati; RRF = Formação Rio do Rasto.

The Rio do Rasto Formation samples also have very different O/S factors. The highest O/S ratio occurs within sample 6B, which is enriched in LREE and HREE. However, sample 7A has a much higher enrichment factor for HREE, but lower in LREE than sample 6B (see Tab. 2). Furthermore, all RRF samples have a negative Ce anomaly. However, sample 6B has a positive Ce anomaly, and 7A has a negative Ce anomaly.

Based on the data in Fig. 8, distribution patterns and degrees of oxidation vary greatly among the stratigraphic units studied. Thus, the comparison between the contents of REE in bones with those in the sedimentary rocks that contain them made it possible to verify that there is no enrichment factor characteristic of REE for the different taxonomic groups or in relation to the type of bone (rib, skull, femur, or other).

Another observation is the fact that the normalization of REE contained in bones by that in sedimentary rocks (O/S) registers some differences from that carried out in relation to chondrite. In the O/S normalization, there is a relative enrichment in Ce in the O2A and O5A samples, which was not recorded in the chondrite normalization.

In summary, it is possible to detect that within analyzed sedimentary matrices (Permian and Triassic ones), those from the Riograndia AZ have the highest REE contents (highlighting La, Ce, Nd, plus Y), whereas those from Hyperodapedon AZ have the lowest REE contents (highlighting Eu, Tb, Ho, Er, Tm, Yb and Lu; Fig. 9A). Looking for fossil bones, those from Permian fauna have, in general, the highest REE contents, highlighting the high levels of Ce e Y and the low levels of La, meanwhile those from the Triassic units have low REE contents, highlighting the high levels of La and the low levels of Ce and Y (Fig. 9C and D).

7. Discussion

7.1 REE complexation

Many anions are responsible for complexation and transport of REE by F, Cl, S, C, P, OH, and organic ligands in fluids. It is worth mentioning that REE used to generate more stable aqueous complexes with monovalent anions in the following order: F^-, OH^-, NO^{3-}, Cl^-, and Br^- (Pearson, 1963), and for the divalent anions as follows: CO^{32-}, SO^{42-}, and PO^{42-} (Williams-Jones *et al.*, 2012), and most of these monovalent anions are present on apatite structure, except NO^{3-} (Toledo & Pereira, 2001). Due to the very weak hydrolysis of REE ions, they predominantly exist either as hydrated ions or as free ions in low-temperature and acidic to weakly basic fluids (Di & Ding, 2024). Environmental factors, such as temperature, pressure, pH, and ligand activity in fluids, can influence the complexation, transport, and deposition of REE.

Despite the influence of F as the main complexing agent on the behavior of REE in fossilization processes in the Permo-Triassic studies of bones, the existence of other anions such as CO^{32-}, CO^2F^{-1}, or even other complexes must also have had a significant influence.

Concerning REE, Y, and F content relationships, the interaction between the bones' phosphate and F promoted its incorporation into hydroxylapatite, probably replacing the OH^- and maybe the oxygen from the tetrahedral site. The tetrahedral oxygen substitution by F in minerals has been already recorded (Valley *et al.*, 1983; Berraho *et al.*, 1994). The incorporation of F in the fossil bones' structure can be corroborated by its higher content in bones than in their sedimentary matrix (Tab. 2). In addition to this, in the studied bones the F contents are highly correlated with REE, LREE ($R^2 = 0.97$) and HREE ($R^2 = 0.94$).

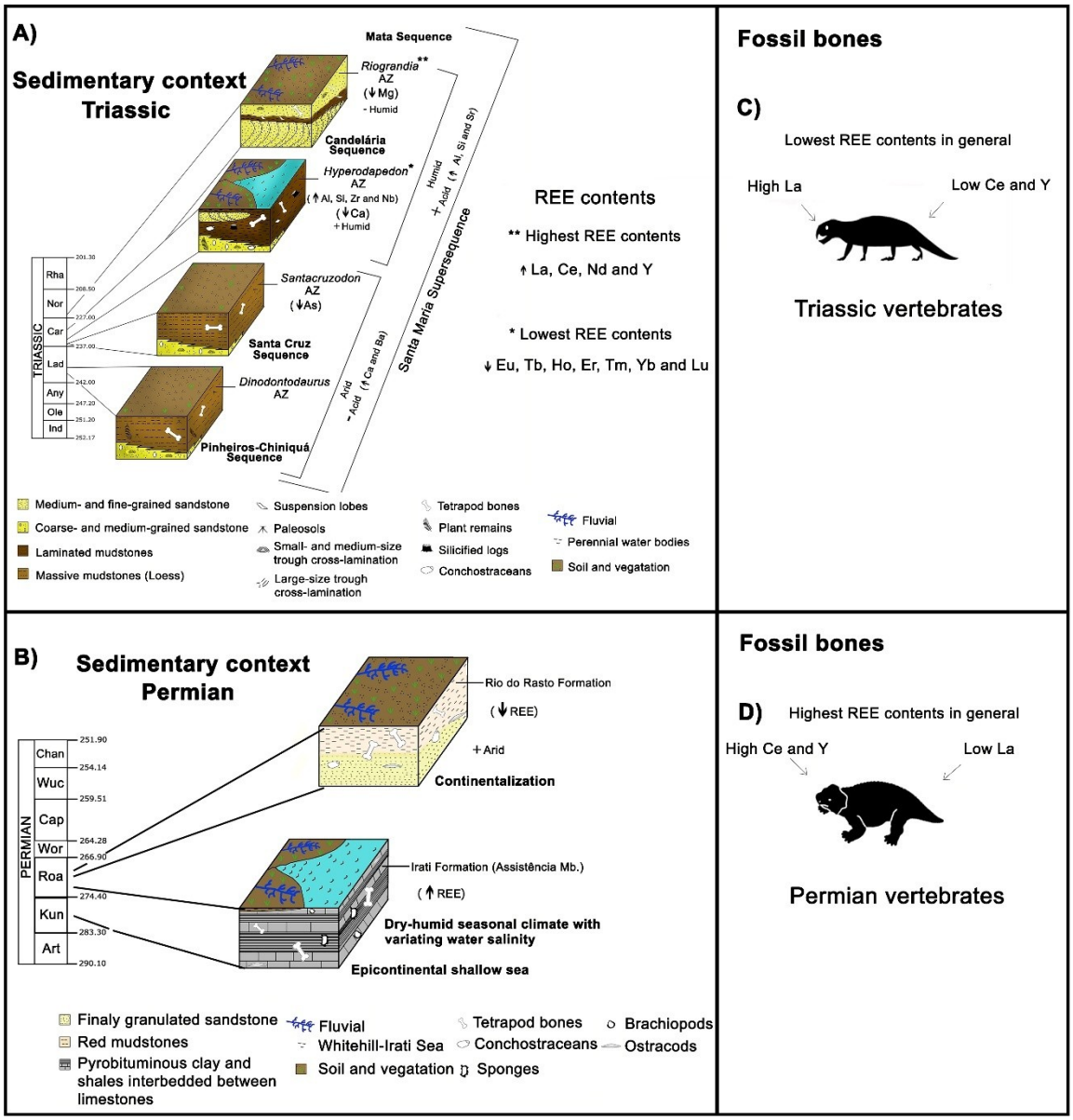

Figure 9. REE distribution synthesis among the analyzed sedimentary matrices and fossil bones.

Figura 9. Síntese da distribuição dos ETR dentre as matrizes sedimentares e ossos fósseis analisados.

The Ca occupies two sites with different coordination numbers (VII and IX) in the apatite structure (Slansky, 1980). Due to the ionic radii similarity (see Shannon, 1976) Ca can be replaced by the REE and Y. Nonetheless REE ionic radii decrease with increasing atomic number, and because of these differences LREEs are easily incorporated in apatite structure. So, all samples studied have higher LREE concentrations than those of HREE, but both accumulate on fossil bones. Furthermore, if we do not consider the Ce and Eu anomalies, which can occur in different oxidation states, the distribution patterns of LREE are less variable than those of HREE. This behavior was confirmed in experimental studies (Fleet & Pan, 1995a; 1995b). Ca can also be replaced by other elements such as Na ($2Ca^{2+}$

= REE^{3+} + Na^{+}), generating a complex charge balance with a great number of stoichiometric balances (Toledo & Pereira, 2001).

The REE complexations, transport, and precipitation depend on the weathering and diagenetic conditions, as the fluid compositions, including the presence of organic matter, iron and manganese oxides, clays, and colloids (Nesbitt, 1979; Erel & Stolper, 1993; Patrick *et al.*, 2004), and salinity, in marine environments (Nozaki *et al.*, 2000). These components associated with the environmental conditions, such as pH and oxidation, are determinants in the precipitation of REE and its concentration in rocks and related fossil bones.

7.2 Fossildiagenetic contexts

To understand the fossil diagenetic context of the studied samples, the following parameters were evaluated: (i) the oxidation from Ce^{+3} to Ce^{+4} and Eu^{+2} to Eu^{+3}; (ii) the acidity by the LREE/HREE ratios, and (iii) the alkalinity by Y/Ho ratios.

The oxidation from Ce^{3+} to Ce^{4+} promotes its precipitation in sediments and lateritic profiles due to the low solubility of its oxidized state (Braun *et al.*, 1990; Zhang & Shields, 2022). It is known that negative Ce anomalies are characteristic of waters from open seas (De Baar *et al.*, 1991; Alibo & Nozaki, 1999; Zhang & Shields, 2022). In this case, the oxidation of Ce^{3+} to Ce^{4+} favors its precipitation, especially because tetravalent oxidation number has low solubility in water (De Baar *et al.*, 1991; Kamber & Webb, 2001). In an estuary from Thailand, a negative Ce anomaly was progressively developed with increasing salinity, being consistent with the continued oxidation of Ce^{3+} to Ce^{4+} (Nozaki *et al.*, 2000).

Extreme conditions are necessary to reduce Eu^{3+} to Eu^{2+}, and it might occur at lower temperatures in significantly reducing and highly alkaline environments (Zhang & Shields, 2022). They also verified the influence of Fe-Mn oxides, phosphates, and organic matter/silicates on Eu depletion, which could reflect the dissolution of specific phases in pore waters. These authors also highlighted that, in general, negative Eu anomalies are uncommon in carbonate rocks, which could indicate strong local effects in restricted seaways or diagenetic exchange with siliciclastic material, implying the need to interpret negative Eu anomalies in carbonate rocks with caution. To relate the degree of negative Eu anomalies with oxidation levels, it is necessary, in future studies, to analyze the samples by cathodoluminescence, whose spectra differentiate Eu^{2+} from Eu^{3+}.

In all the analyzed sedimentary rocks from the SMS, Ce does not present a positive anomaly, and Eu always has a negative anomaly, which suggests reducing geochemical conditions for this unit. In its fossil bones, only the sample O3B (*Hyperodapedon* AZ, Rhynchosaur from Vale do Sol; see Chart 1) has a positive Ce anomaly, which indicates that it was exposed to subaerial conditions at least at some point of its fossidiagenesis. Recently, a biostratigraphic refinement was proposed for the *Hyperodapedon* AZ, with the Vale do Sol outcrops serving as the basis for this new proposal (Scartezini *et al.*, 2025). According to these authors, this assemblage zone can be subdivided into two subzones, from the base to the top: the *Hyperodapedon* Acme Zone and the *Exaeretodon* sub-AZ. In addition, a *Siriusgnathus* + *Teyumbaita* level was identified within the *Hyperodapedon* AZ

(at its top), although further data are needed to confirm this. All the records of rhynchosaurs from the Vale do Sol outcrops were encompassed within *Hyperodapedon* Acme Zone, which includes our sample set O3B/S3B (which came from Degrau Site, Scartezini, C. personal communication). Although some specimens from that outcrop have observations about their collection (e.g., UFRGS-PV-1204-T - rhynchosaur vertebra - *ex situ*; UFRGS-PV-1209-T - rhynchosaur left humerus - *in situ*; UFRGS-PV-1210-T - rhynchosaur right humerus - *in situ*; UFRGS-PV-1332-T - rhynchosaur vertebra - *ex situ*), according to Scartezini *et al.* (2025), there is no information concerning the specimen UFRGS-PV-1206-T (here O3B). Therefore, the hypotheses of pre- and post-burial reworking cannot be ruled out based on the available information.

In the analyzed sedimentary rocks from the IF, there were no positive Ce and Eu anomalies, which indicates that within this formation, the fossilization process also occurred in a reducing environment. The bones from this formation have differences in relation to the sedimentary rocks that host them. These variations are also recorded in the geochemical behavior of Er (negative anomaly in sample O5A and positive in O5B), and the exact meaning of these alterations can only be fully understood with more analyses on a greater number of samples.

Regarding the sedimentary rocks of the RRF, significant changes in cerium contents were observed. Sample S6A has a high positive anomaly, S6B has almost no anomaly, and S7A has a negative anomaly. Similar trends are recorded in the fossil bones of this formation. It is noteworthy that the RRF samples came from geographically very distant locations and, therefore, each sample must reflect different redox contexts.

HREE are associated with basic and carbonate-bearing alkaline waters (high pH) and LREE with acidic and neutral waters (low pH), being that acid environments include waterlogged settings such as swampy areas (Johannesson & Zhou, 1997; Suarez, 2004; Martin *et al.*, 2005). All studied sedimentary rocks and bones have high LREE/HREE ratios, meaning that the environments of fossilization were acidic (low pH). Despite this, carbonates are registered by nodules in sediments and inclusions of calcite in pores and Haversian channels of fossilized bones in some of these units (Holz & Schultz, 1998; Reichel *et al.*, 2005; Horn *et al.*, 2013). These nodules and inclusions were already confirmed by scanning electron microscopy (SEM) and infrared analysis carried out by Corecco *et al.* (2023) and Corecco (2024). Although the modal calcite contents are relatively small, the presence of CO_3^{2-} must have interfered with the REE transport processes, promoting replacements in the bones during fossilization and diagenesis. The different degrees of acidity are mainly due to the great influence of fluorine on the fossilization processes, which was previously reported by Corecco *et al.* (2020, 2021) that analyzed fossil bones and their sedimentary rocks from the same Permian and Triassic units contemplated in this study. Corecco *et al.* (2021) detected that fluorine has the following averages in these units: 0.93 Wt% = Permian fossil bones; 0.17 Wt% = Permian sedimentary rocks, and 0.76 Wt% = Triassic fossil bones; 0.13 Wt% = Triassic sedimentary rocks. The large variations in the LREE/HREE ratios confirm that other factors contributed to these differences. The influence of iron

oxyhydroxides, such as hematite and goethite, observed in the samples studied must have contributed to the REE concentrations. Hematite was already detected within and attached to the surface of some fossils of the SMS (Holz & Schultz, 1998).

Another point that attests different degrees of acidity within the Santa Maria Supersequence is the clay minerals content from its rocks that suggests an arid to semi-arid climate (e.g., illite/smectite mixed layers and illite). In Arroio Moirão Graben, one of the six isolated Gondwana Units over the Sul-riograndense Shield, the clay minerals content is confined to kaolinite, implying humid conditions (Rodrigues *et al.*, 2019). Differences in clay mineral assemblages for these sedimentary units exemplify distinct diagenetic and/or climate conditions.

When observing the LREE/HREE ratios of the different stratigraphic units, it is possible to verify that for SMS, they vary from 6.14 to 8.94 in sedimentary rocks and from 5.73 to 10.42 in fossil bones, meaning that fossilization, at least in its beginning, occurs in acidic or neutral environments (low pH), possibly due to the decomposition of the organic matter. In the sedimentary rocks of the Irati Formation, these values vary from 4.32 to 8.93, and those of the bones contained therein have values between 8.78 and 10.50, indicating that they also come from acidic or neutral environments. Furthermore, in the fossil bones of this formation, samples 5A and 5B have higher LREE/HREE ratios, indicating that the environment was more acidic than that of sample 5C. Therefore, there are variations in acidity within the formation itself, and even in samples from the same location. Similar conditions occurred in the RRF, where values in sedimentary rocks varied between 4.56 and 7.70 and in fossil bones from 2.32 to 7.51. However, sample 7A (*Provelosaurus*) deserves to be highlighted due to the significant reduction in the LREE/HREE ratio, indicating that in this environment, the fossilization conditions were much less acidic than the others. It is worth mentioning that despite these units having sedimentary features (e.g., carbonate nodules and inclusions, shales) suggesting reducing conditions, these LREE/HREE ratios indicating acid environments can represent microenvironmental modifications (e.g., pH) triggered by the decomposition of organic matter in the beginning of fossildiagenetic process, which is when most of the REE are incorporated (Trueman & Tuross, 2002). A similar situation was proposed for the Santana Group biota (Lower Cretaceous) of the Araripe Basin, Brazil (Martill *et al.*, 1988). According to these authors, the HCO_3^- released into the microenvironment during the decomposition of the organisms may have altered the local pH and contributed to the deposition of Ca^{2+} and $CaCO_3^{2-}$ over the carcasses, which may have favored concretion formation in that setting. Specimens encrusted with thin dark red to blackish layers of iron (predominantly) and manganese oxides, and/or involved by carbonate concretions, have also been observed in SMS assemblage zones (e.g., *Santacruzodon* AZ; Reichel *et al.*, 2005; Battista *et al.*, 2024a). These encrustations appear to be unaffected by the volumetric expansion that occurred during permineralization processes (Holz & Schultz, 1998).

According to Bau & Dulski (1999), Y behaves like the HREE and its mobility is different from the LREE, such as Ce. Aqueous solutions have higher Y/Ho ratios that

increases in thermal systems (Bau & Dulski, 1995), but Ho is removed from seawater twice as fast as Y due to differences in surface complexation behavior (Nozaki *et al.*, 1997). Although Y/Ho is a useful monitor for the differentiation between marine and non-marine deposits (Bau, 1996; Nothdurft *et al.*, 2004), this ratio in aqueous solutions is a result of the REE-F complexes and the stability increases with the atomic number, which was evidenced in mono fluorine as (REE, Y)F^{2+} where Y acts as a heavy pseudolanthanide, such Lu (Bau & Dulski, 1995). Furthermore, enrichments in Y and Ho are often associated with the presence of organic matter in carbonates (Nozaki *et al.*, 1997). In the estuarine mixing zone from Thailand, the Y/Ho ratios are unclear (Nozaki *et al.*, 2000). According to Bau & Dulski (1995), the influence of softer ligands, such as carbonate complexes, forces Y to act as a light to medium pseudolanthanide. The lack of correlation between the Y/Ho ratios (chondrite-normalized) and the F content is commonly related to the presence of other complexing agents, such as carbonate and organic matter. These complexing agents interfere with the transport and fixation of Y and Ho in sedimentary rocks and fossil bones, making the Y/Ho-F-CO_3^{2-} relationship extremely complex and dependent on local geochemical conditions.

Non-normalized Y/Ho ratios with values between 60 and 90 indicate the predominance of open marine systems, and those below 60 record the influence of continental inputs in proximal environments or restricted seas (Frimmel, 2009). In the SMS sedimentary rocks, the Y/Ho ratio of the non-standardized tenors of these elements varies from 26.59 to 46.22, while in the bones of this supersequence it ranges from 29.27 to 34.60. In the IF, these values in bones vary between 34.06 and 39.88, and in sedimentary rocks between 30.18 and 38.00. In the sedimentary rocks of the Rio do Rasto Formation (RRF), these ratio values range from 24.39 to 30.48, while in the bones of this formation from 24.79 to 34.85. Therefore, these values are in accordance with those established for the sedimentary rocks of the SMS and RRF, which are continental. For IF, which has marine context, values lower than 60 indicate the great influence of continental sedimentation.

Statistical correlations of Y with ΣREE, ΣLREE, ΣHREE, and Ho in the studied sedimentary rocks have very high values (0.99) in all cases. This means that Y behaves like a REE in sedimentary rocks. However, these correlations in fossil bones are low for ΣREE (0.58) and ΣLREE (0.48), but high for ΣHREE (0.97) and Ho (0.99). It means that Y also behaves like a HREE in bones. Furthermore, all fossil bone samples show a positive Y anomaly when normalized by the sedimentary rocks that contain them and do not show a defined distribution pattern. Due to this, it does not have a significant correlation with different degrees of oxidation or reduction.

A small modal amount of secondary phosphate of LREE (probably florencite) crystalized in the bone's pores during fossilization processes and diagenesis, may be one of the reasons for the lack of high correlation between ΣREE and ΣLREE in the bones studied. The presence of florencite was already inferred within some SMS teeth by Corecco *et al* (2023).

Furthermore, it must be considered that by changing the normalization pattern, differences in interpretations regarding the behavior of the elements may occur and, consequently, interpretations regarding the degree of oxidation of Ce and Eu must also be interpreted with caution because the values of Ce^{+3} and Ce^{+4} and Eu^{+2} and Eu^{+3} were not quantified.

8. Conclusions

In summary, our data highlighted that the REE contents in fossil bones can be up to hundreds of times greater than those of their sedimentary host rocks. The high statistical correlations between REE and Y with F in the bone samples indicate that F is the main anion in the complexation of these elements. Y also has a high correlation with REE in fossil bones and in sedimentary host rocks, but no correlation was verified between REE or Y with F in the sedimentary rocks. Thus, it is possible to conclude that Y behaves as an HREE (R^2 = 0.95) and easily replaces Ca (diadochic substitution) in the apatite structure. In addition to F^-, other ions such as CO_3^{2-}, OH^- influenced the fossilization processes. Because of local geochemical conditions, the distribution patterns of REE in all studied bones are similar to those of their sedimentary host rocks. This and the high statistical correlations among REE contents in the fossil bones and their sedimentary host rocks attest that there was no significant transport of bones during fossilization, meaning that the fossil bones studied represent peripheral assemblages (were not transported far from where they were preserved; adapted from Araújo-Júnior, 2016).

The extreme variations in REE content indicate that the geochemical processes involved in fossilization were very different, and, therefore, it is not possible to know the origin of a given fossil based solely on its REE content. The comparison of the REE, LREE, and HREE contents between the sedimentary rock samples and those of the host fossils did not allow for differentiating the Permian stratigraphic units from those of the Triassic. Furthermore, in bones, LREE substitutes for Ca more readily than HREE because the environments studied are acidic, at least at the beginning of the preservation process that was recorded.

The Y/Ho ratio values lower than 60 obtained for sedimentary rocks from SMS and RRF agree with those established for continental environments, whereas values below 60 indicate that FI (that had a marine context) can indicate both the influence of continental sedimentation or the generation in a restricted sea context, which agrees with the previous works conducted in these units.

Despite these units having sedimentary features that suggest reducing conditions (e.g., carbonate nodules and inclusions, shales), the obtained LREE/HREE ratios indicate acid environments, which can represent microenvironmental modifications (e.g., pH) triggered by the decomposition of organic matter at the beginning of the fossil diagenetic process.

As final conclusions, it is possible to state that the small number of samples studied, and the wide variety of bone types associated with geographically distant and different

environments resulted in varied distribution patterns of REE and Y. These differences record the large and significant variations in fossilization processes, even in fossils from the same stratigraphic level. Therefore, based solely on the contents and patterns of the REE and Y, it was not possible to identify the place of origin or even the type of environment of the fossils studied. It is not possible to use exclusively REE and/or Y as a forensic tool to identify materials removed from the studied sites without collecting more data. So, considering the small number of samples available for this work in the different outcrops, it is suggested that future studies be carried out with greater statistical representation.

Acknowledgements: We are thankful to Conselho Nacional de Desenvolvimento Científico e Tecnológico - CNPq (grants 476868/2010-6, 406779/2021-0, 308515/2023 to M.B.S.; INCT Paleovert 406902/2022-4 to M.B.S. and L.C.) and to Fundação de Amparo à Pesquisa do Estado do Rio de Janeiro – FAPERJ (grant E-26/204.181/2024 to M.B.S). We also thank Carlos Nunes Rodrigues (Museu Aristides Carlos Rodrigues) for making the specimen MMACRPV012T available to this study and Cristina Vega Dias (Universidade Federal do Paraná) for the specimen UFPR0150PV.

Author statement: P.A.V.P., L.C., V.P.P., and M.B.S. wrote the first draft of the manuscript. L.C., V.P.P., and P.A.V.P. prepared figures 1 to 10. P.A.V.P., V.P.P., L.C., and M.B.S. reviewed the literature referenced in this study. All the authors revised and improved the final draft before submission.

Conflict of Interest: The authors declare that there is no conflict of interest.

References

Abdala, F., Barberena, M.C. & Dornelles, J.F. 2002. A new species of the traversodontid cynodont Exaeretodon from the Santa Maria Formation, Middle/Late Triassic) of southern Brazil. *Journal of Vertebrate Paleontology*, 22: 313-325. https://doi.org/10.1671/0272-4634(2002)022[0313:ANSOTT]2.0.CO;2

Adami-Rodrigues, K., Pazinato, P. & Damiani-Pinto, I. 2016. New species of Pygocephalomorpha (Crustacea) from the Irati Formation, Paraná Basin, RS, southern Brazil. *Revista Brasileira de Paleontologia*, 19(3): 389-400. https://doi.org/10.4072/rbp.2016.3.04

Alibo, D.S. & Nozaki, Y. 1999. Rare earth elements in seawater: particle association, shale-normalization, and Ce oxidation. *Geochimica et Cosmochimica Acta*, 63(3–4): 363-372. https://doi.org/10.1016/S0016-7037(98)00279-8

Andreis, R.R., Bossi, G.E. & Montardo, D.K. 1980. O Grupo Rosário do Sul (Triássico) no Rio Grande do Sul. In: *Anais...* XXXI CONGRESSO BRASILEIRO DE GEOLOGIA, p. 659-673.

Anders, E. & Grevesse, N. 1989. Abundances of the elements: Meteoritic and solar. *Geochimica et Cosmochimica Acta*, 53(1): 197-214. https://doi.org/10.1016/0016-7037(89)90286-X

Anderson, P.E., Benton, M.J., Trueman, C.N., Paterson, B.A. & Cuny, G. 2007. Palaeoenvironments of vertebrates on the southern shore of Tethys: the nonmarine Early Cretaceous of Tunisia. *Palaeogeography, Palaeoclimatology, Palaeoecology*, 243(1–2): 118-131. https://doi.org/10.1016/j.palaeo.2006.07.015

Araújo, D.C. 1985. Sobre Pareiasaurus americanus sp. nov., do Permiano superior do Rio Grande do Sul, Brasil, I–diagnose específica. *Anais da Academia Brasileira de Ciências*, 57: 63-66.

Araújo, L.M. 2001. *Análise da expressão estratigráfica dos parâmetros de geoquímica orgânica e inorgânica nas sequências deposicionais Irati*. Porto Alegre, 307 p. Unpublished PhD thesis, Programa de Pós-graduação em Geociências, Universidade Federal do Rio Grande do Sul, Porto Alegre, 2v.

Araújo-Júnior, H.I. 2016. Classifying vertebrate assemblages preserved in Quaternary tank deposits: Implications for vertebrate taphonomy and paleoecology. Palaeogeography, *Palaeoclimatology, Palaeoecology*, 445: 147-152. https://doi.org/10.1016/j.palaeo.2015.12.025

Araújo-Júnior, H.I. & Bisarro-Júnior, M.C. 2017. Tafonomia de vertebrados em ambientes continentais. In: Horodyski, R.S. & Erthal, F. (Eds.). *Tafonomia - Métodos, processos e aplicação*. Curitiba, Editora CRV, p. 175-236.

Azevedo, K.L., Schemiko, D.C.B., Soares, M.B., Vega, C.S. & Vesely, F.F. 2018. The São Jerônimo da Serra Site, Rio do Rasto Formation (Middle/Upper Permian), Paraná Basin, Brazil: faciological and taphonomic context. Brazilian *Journal of Geology*, 48(4): 821-837. https://doi.org/10.1590/2317-4889201820170129

Barberena, M.C. & Dias, E.V. 1998. On the presence of a short-snouted rhinesuchoid amphibian in the Rio do Rasto formation (Late Permian of Paraná Basin, Brazil). *Anais da Academia Brasileira de Ciências*, 70: 465-468.

Battista, F. & Schultz, C.L. 2022. Rhizoliths, Rhizocretions, and the anthropogenic Biases: a case study from the upper Triassic beds of southern Brazil. In: THE 80TH ANNIVERSARY OF EFREMOV'S TAPHONOMY, 9TH TAPHOS INTERNATIONAL MEETING ON TAPHONOMY AND FOSSILIZATION, *Journal of Taphonomy*, 16(1-4), p. 13-14.

Battista, F., Ribeiro, A.M., Melo, T.P. & Schultz, C.L. 2024a. A reinterpretation of taphonomy and palaeoecology of the early Carnian Santacruzodon assemblage zone type-locality (Santa Maria supersequence), Brazil. *Palaeogeography, Palaeoclimatology, Palaeoecology*, 639: 112080. https://doi.org/10.1016/j.palaeo.2024.112080

Battista, F., Martinelli, A.G., Ribeiro, A.M., De Andrade, M.B. & Schultz, C.L. 2024b. First record of rhynchosaurs (Archosauromorpha: Rhynchosauria: Hyperodapedontinae) from the early Late Triassic Santacruzodon Assemblage Zone of the Santa Maria Supersequence, Brazil. *The Anatomical Record*, 308(8): 2141-2159. https://doi.org/10.1002/ar.25589

Bau, M., 1996. Controls on the fractionation of isovalent trace elements in magmatic and aqueous systems: evidence from Y/Ho, Zr/Hf, and lanthanide tetrad effect. *Contributions to Mineralogy and Petrology*, 123: 323-333. https://doi.org/10.1007/s004100050159

Bau, M. & Dulski, P. 1995. Comparative study of yttrium and rare-earth element behaviours in fluorine-rich hydrothermal fluids. *Contributions to Mineralogy and Petrology*, 119: 213-223. https://doi.org/10.1007/BF00307282

Bau, M. & Dulski, P. 1999. Comparing yttrium and rare earths in hydrothermal fluids from the Mid-Atlantic Ridge: implications for Y and REE behaviour during near-vent mixing and for the Y/Ho ratio of Proterozoic seawater. *Chemical Geology*, 155(1–2): 77-90. https://doi.org/10.1016/S0009-2541(98)00142-9

Berraho, M., Vegas, A., Martínez-Ripoll, M & Rafiq, M. 1994. A copper monofluorophosphate, Cu $(H_2O)_2$ $(NH_4)_2$ $(PO_3F)_2$. *Acta Crystallographica*, C50: 666-668. https://doi.org/10.1107/S0108270193010789

Bonaparte, J.F. & Barberena, M.C. 2001. On two advanced carnivorous cynodonts from the Late Triassic of southern Brazil. *Bulletin of the Museum of Comparative Zoology*, 156: 59-80.

Boos, A.D.S., Schultz, C.L., Vega, C.S. & Aumond, J.J. 2013. On the presence of the Late Permian dicynodont Endothiodon in Brazil. *Palaeontology*, 56(4): 837-848. https://doi.org/10.1111/pala.12020

Boos, A.D.S., Kammerer, C.F., Schultz, C.L. & Paes Neto, V.D. 2015. A tapinocephalid dinocephalian (Synapsida, Therapsida) from the Rio do Rasto Formation (Paraná Basin, Brazil): taxonomic, ontogenetic and biostratigraphic considerations. *Journal of South American Earth Sciences*, 63: 375-384. https://doi.org/10.1016/j.jsames.2015.09.003

Boos, A.D.S., Kammerer, C.F., Schultz, C.L., Soares, M.B. & Ilha, A.L.R. 2016. A new dicynodont (Therapsida: Anomodontia) from the Permian of southern Brazil and its implications for bidentalian origins. *PLoS One*, 11(5): e0155000. https://doi.org/10.1371/journal.pone.0155000

Braun, J-J., Pagel, M., Muller, J-P, Bilong, P., Michard, A. & GUILLET, B. 1990. Cerium anomalies in lateritic profiles. *Geochimica et Cosmochimica Acta*, 54(3): 781-795. https://doi.org/10.1016/0016-7037(90)90373-S

Cabreira, S.F., Schultz, C.L., Bittencourt, J., Soares, M.B., Fortier, D.C., Silva, L.R. & Langer, M.C. 2011. New stem-sauropodomorph (Dinosauria, Saurischia) from the Triassic of Brazil. *Naturwissenschaften*, 98: 1035-1040. https://doi.org/10.1007/s00114-011-0858-0

Cabreira, S.F., Kellner, A., Dias-da-Silva, S., Roberto da Silva, L., Bronzati, M., Marsola, J.C., Müller, R.T., Bittencourt, J.S. & Batista, B. 2016. A Unique Late Triassic Dinosauromorph Assemblage Reveals Dinosaur Ancestral Anatomy and Diet. *Current Biology*, 26(22): 3090-3095. doi:10.1016/j.cub.2016.09.040

Cisneros, J.C., Abdala, F., Rubidge, B.S., Dentzien-Dias, D. & Bueno, A.O. 2011. Dental Occlusion in a 260-Million-Year-Old Therapsid with Saber Canines from the Permian of Brazil. *Science*, 331: 1603-1605. https://doi.org/10.1126/science.1200305

Cisneros, J.C., Abdala, F., Atayman-Güven, S., Rubidge, B.S., Celâl Sxengör, A.M. & Schultz, C.L. 2012. Carnivorous dinocephalian from the Middle Permian of Brazil and tetrapod dispersal in Pangea. *PNAS*, 109(5): 1584-1588. ttps://doi.org/10.1073/pnas.111597510

Clements, T., Purnell, M.A. & Gabbott, S.E. 2022. Experimental analysis of organ decay and pH gradients within a carcass and the implications for phosphatization of soft tissues. *Palaeontology*, 65(4): e12617. https://doi.org/10.1111/pala.12617

Cohen, K.M., Finney, S.C., Gibbard, P.L. & Fan, J.-X. 2024. (c) *International Commission on Stratigraphy*, December 2024.

Corecco, L., 2024. *Reconstituição Paleoambiental e Paleoecológica do Triássico do Rio Grande do Sul com Base em Evidências Geoquímicas em dentes de Tetrápodes*. Porto Alegre, 321p. Unpublished PhD thesis, Programa de Pós-graduação em Geociências, Universidade Federal do Rio Grande do Sul.

Corecco, L., Pereira, V.P., Soares, M.B. & Schultz, C.L. 2020. Geochemical study of the vertebrate assemblage zones of the Santa Maria supersequence (Middle to Late Triassic), Paraná Basin, Brazil. Brazilian *Journal of Geology*, 50(4): e20200014. https://doi.org/10.1590/2317-4889202020200014

Corecco, L., Pereira, V.P., Soares, M.B. & Schultz, C.L. 2021. Geochemical study on fossil vertebrates from some specific Permian and Triassic beds of the Paraná Basin (Brazil): A preliminary approach. *Journal of South American Earth Sciences*, 110, 103362. https://doi.org/10.1016/j.jsames.2021.103362

Corecco, L., Pereira, V.P., Erthal, F. & Schultz, C.L. 2023. Aspectos Tafonômicos de Dentes Isolados de Arcossauros da Supersequência Santa Maria. In: *Anais...* II SIMPÓSIO BRASILEIRO DE TAFONOMIA, Porto Alegre, p. 22-22.

Daculsi, G., Bouler, J.-M. & Legeros, R.Z. 1997. Adaptive crystal formation in normal and pathological calcifications in synthetic calcium phosphate and related biomaterials. *International Review of Cytology*, 172: 129-191. https://doi.org/10.1016/s0074-7696(08)62360-8

De Baar, H.J.W., Schijf, J. & Byrne, R.H. 1991. Solution chemistry of the rare earth elements in seawater. *European Journal of Solid State and Inorganic Chemistry*, 28: 357-373.

Di, J. & Ding, X. 2024. Complexation of REE in Hydrothermal Fluids and Its Significance on REE Mineralization. Minerals, 14(6): 531. https://doi.org/10.3390/min14060531

Dia, A., Gruau, G., Olivie-Lauquet, G., Riou, C., Molenat, J. & Curmi, P. 2000. The distribution of rare earth elements in groundwaters: Assessing the role of source-rock composition, redox changes and colloidal particles. *Geochimica et Cosmochimica Acta*, 64(24): 4131-4151. https://doi.org/10.1016/S0016-7037(00)00494-4

Dias, E.V. & Barberena, M.C. 2001. A temnospondyl amphibian from the Rio do Rasto formation, upper Permian of southern Brazil. *Anais da Academia Brasileira de Ciências*, 73: 135-143. https://doi.org/10.1590/S0001-37652001000100011

Dias-da-Silva, S., Pinheiro, F., Da-Rosa, Á.A.S., Martinelli, A.G., Schultz, C.L., Silva-Neves, E. & Modesto, S.P. 2017. Biostratigraphic reappraisal of the lower Triassic Sanga do Cabral Supersequence from South America, with a description of new material attributable to the parareptile genus Procolophon. *Journal of South American Earth Sciences*, 79: 281-296. https://doi.org/10.1016/j.jsames.2017.07.012

Elderfield, H. & Pagett, R. 1986. Rare earth elements in ichthyoliths: variations with redox conditions and depositional environment. *Science of The Total Environment*, 49: 175-197. https://doi.org/10.1016/0048-9697(86)90239-1

Elliott, J.C. 2002. Calcium phosphate biominerals. In: Kohn, M.J., Rakovan, J. & Hughes, J.M. (Eds.). *Reviews in Mineralogy and Geochemistry*, 48(1), p. 427- 453. https://doi.org/10.2138/rmg.2002.48.11

Erel, Y. & Stolper, E.M. 1993. Modeling of rare-earth element partitioning between particles and solution in aquatic environments. *Geochimica et Cosmochimica Acta*, 57(3): 513-518. https://doi.org/10.1016/0016-7037(93)90363-2

Ernesto, M., Demarco, P.N., Xavier, P.A., Sanchez, L.B., Schultz, C.L. & Piñeiro, G. 2020. Age constraints on the Paleozoic Yaguarí-Buena Vista succession from Uruguay: paleomagnetic and paleontologic information. *Journal of South American Earth Sciences*, 98: 102489. https://doi.org/10.1016/j.jsames.2019.102489

Feldmann, R.M. 1989. Selection of Appropriate Preparation Techniques. In: Feldmann, R.M., Chapman, R.E. & Hannibal, J.T. (Eds.). *Paleotechniques. The Paleontological Society Special Publication*, 4, p. 24-29.

Fleet, M.E. & Pan, Y. 1995a. Crystal chemistry of rare earth elements in fluorapatite and some calc-silicates. *European Journal of Mineralogy*, 7(3): 591-606.

Fleet, M.E. & Pan, Y. 1995b. Site preference of rare earth elements in fluorapatite. *American Mineralogist*, 80(3–4): 329-335. https://doi.org/10.2138/am-1995-3-415

Francischini, H., Dentzien-Dias, P., Guerra-Sommer, M., Menegat, R., Santos, J.O.S., Manfroi, J. & Schultz, C.L. 2018. A middle Permian (Roadian) lungfish aestivation burrow from the Rio do Rasto Formation (Paraná Basin, Brazil) and associated U-Pb dating. *Palaios*, 33(2): 69-84. https://doi.org/10.2110/palo.2017.050

Frimmel, H.E. 2009. Trace element distribution in neoproterozoic carbonates as palaeoenvironmental indicator. *Chemical Geology*, 258(3–4): 338-353. https://doi.org/10.1016/j.chemgeo.2008.10.033

German, C.R. & Elderfield, H. 1990. Application of the Ce anomaly as a redox indicator: the ground rules. *Paleoceanography*, 5(5): 823-833. https://doi.org/10.1029/PA005i005p00823

Goldberg, K. & Humayun, M. 2016. Geochemical paleoredox indicators in organic-rich shales of the Irati Formation, Permian of the Paraná Basin, southern Brazil. Brazilian *Journal of Geology*, 46: 377-393. https://doi.org/10.1590/2317-4889201620160001

Grandjean-Lécuyer, P., Feist, R. & Albarède, F. 1993. Rare earth elements in old biogenic apatite. *Geochimica et Cosmochimica Acta*, 57(11): 2507-2514. https://doi.org/10.1016/0016-7037(93)90413-Q

Gruau, G., Dia, A., Olivié-Lauquet, G., Davranche, M. & Pinay, G. 2004. Controls on the distribution of rare earth elements in shallow groundwaters. *Water Research*, 38(16): 3576-3586. https://doi.org/10.1016/j.watres.2004.04.056

Guerrini, V.B., Matos, S.A., Rohn, R., Varejão, F.G., Warren, L.V. & Simões, M.G. 2020. The last chapter of 30 million years of molluscan evolution: Permian non-marine bivalves of the Rio do Rasto Formation, Paraná Basin, Brazil. *PalZ*, 94(3): 487-512. https://doi.org/10.1007/s12542-019-00455-0

Haskin, L.A. & Frey, F.A. 1966. Dispersed and Not-So-Rare Earths. *Science*, 152(3720): 299-314. https://doi.org/10.1126/science.152.3720.299

Haskin, L.A., Wildeman, T.R. & Haskin, M.A. 1968. An accurate procedure for the determination of the rare earths by neutron activation. *Journal of Radioanalytical and Nuclear Chemistry*, 1: 337-348. https://doi.org/10.1007/BF02513689

Haskin, M.A. & Haskin, L.A. 1966. Rare earths in European shales: a redetermination. *Science*, 54(3748): 507-509. https://doi.org/10.1126/science.154.3748.507

Hedges, R.E.M. 2002. Bone diagenesis: an overview of processes. *Archaeometry*, 44(3): 319-328. https://doi.org/10.1111/1475-4754.00064

Herwartz, D., Tütken, T., Münker, C., Jochum, K.P., Stoll, B. & Sander, P.M. 2011. Timescales and mechanisms of REE and Hf uptake in fossil bones. *Geochimica et Cosmochimica Acta*, 75(1): 82-105. https://doi.org/10.1016/j.gca.2010.09.036

Holz, M. & Schultz, C.L. 1998. Taphonomy of the south Brazilian Triassic herpetofauna: fossilization mode and implications for morphological studies. *Lethaia*, 31(4): 335-345. https://doi.org/10.1111/j.1502-3931.1998.tb00523.x

Holz, M. & Souto-Ribeiro, A. 2000. Taphonomy of the south-Brazilian Triassic vertebrates. Brazilian *Journal of Geology*, 30(3): 491-494. https://doi.org/10.25249/0375-7536.2000303491494

Holz, M., França, A.B., Souza, P.A., Iannuzzi, R. & Rohn, R. 2010. A stratigraphic chart of the Late Carboniferous/Permian succession of the eastern border of the Paraná Basin, Brazil, South America. *Journal of South American Earth Sciences*, 29(2): 381-399. https://doi.org/ 10.1016/j.jsames.2009.04.004

Horn, B.L.D., Pereira, V.P. & Schultz, C.L. 2013. Calcretes of the Santa Maria Supersequence, Middle Triassic, Rio Grande do Sul, Brazil: classification, genesis and paleoclimatic implications. *Palaeogeography, Palaeoclimatology, Palaeoecology*, 376: 39-47. https://doi.org/10.1016/j.palaeo.2013.02.013

Horn, B.L.D., Melo, T.M., Schultz, C.L., Philipp, R.P., Kloss, H.P. & Goldberg, K. 2014. A new third-order sequence stratigraphic framework applied to the Triassic of the Parana Basin, Rio Grande do Sul, Brazil, based on structural, stratigraphic and paleontological data. *Journal of South American Earth Sciences*, 55: 123-132. https://doi.org/10.1016/j.jsames.2014.07.007

Horn, B.D., Goldberg, K. & Schultz, C.L. 2018a. A loess deposit in the Late Triassic of southern Gondwana, and its significance to global paleoclimate. *Journal of South American Earth Sciences*, 81: 189-203. https://doi.org/10.1016/j.jsames.2017.11.017

Horn, B.D., Goldberg, K. & Schultz, C.L. 2018b. Interpretation of massive sandstones in ephemeral fluvial settings: A case study from the Upper Candelária Sequence (Upper Triassic, Paraná Basin, Brazil). *Journal of South American Earth Sciences*, 81: 108-121.https://doi.org/10.1016/j.jsames.2017.10.009

Huene, F.V. 1942. *Die fossilen Reptilien des Sudamerikanischen Gondwanalandes. Ergebnisse der Sauriergrabungen in Sudbrasilien, 1928/1929*. Munchen: C. H. Beck'she. 332 p.

Johannesson, K.H. & Zhou, X. 1997. Geochemistry of the rare earth elements in natural terrestrial waters: a review of what is currently known. *Chinese Journal of Geochemistry*, 16: 20-42. https://doi.org/10.1007/BF02843369

Johannesson, K.H., Zhou, X., Guo, C., Stetzenbach, K.J. & Hodge, V.F. 2000. Origin of rare earth element signatures in groundwaters of circumneutral pH from southern Nevada and eastern California, USA. *Chemical Geology*, 164(3–4): 239-257. https://doi.org/10.1016/S0009-2541(99)00152-7

Kamber, B.S. & Webb, G.E. 2001. The geochemistry of late Archaean microbial carbonate: implications for ocean chemistry and continental erosion history. *Geochimica et Cosmochimica Acta*, 65(15): 2509-2525. https://doi.org/10.1016/S0016-7037(01)00613-5

Kellner, A.W.A., Holgado, B., Grillo, O., Pretto, F.A., Kerber, L., Pinheiro, F.L., Soares, M. B., Schultz, C.L., Lopes, R.T., Araújo, O. & Müller, R.T. 2022. Reassessment of Faxinalipterus minimus, a purported Triassic pterosaur from southern Brazil with the description of a new taxon. *PeerJ*, 10: e13276. https://doi.org/10.7717/peerj.13276

Koenig, A.E., Rogers, R.R. & Trueman, C.N. 2009. Visualizing fossilization using laser ablation - inductively coupled plasma mass spectrometry maps of trace elements in Late Cretaceous bones. *Geology*, 37(6): 511-514. https://doi.org/10.1130/G25551A.1

Kohn, M.J. 2008. Models of diffusion-limited uptake of trace elements in fossils and rates of fossilization. *Geochimica et Cosmochimica Acta*, 72(15): 3758-3770. https://doi.org/10.1016/j.gca.2008.05.045

Kohn, M.J., Schoeninger, M.J. & Barker, W.W. 1999. Altered states: Effects of diagenesis on fossil tooth chemistry. *Geochimica et Cosmochimica Acta*, 63(18): 2737-2747. https://doi.org/10.1016/S0016-7037(99)00208-2

Lacerda, M.B., Schultz, C.L. & Bertoni-Machado, C., 2015. First "Rauisuchian" archosaur (Pseudosuchia, Loricata) for the Middle Triassic Santacruzodon Assemblage Zone (Santa Maria Supersequence), Rio Grande do Sul State, Brazil. *PloS One*, 10(2): e0118563. https://doi.org/10.1371/journal.pone.0118563

Langer, M.C. 2000. The first record of dinocephalian in south America: Late Permian (Rio do Rasto Formation) of the Paraná Basin, Brazil. *Neues Jahrbuch für Geologie und Paläontologie*, 215(1): 69-95. https://doi.org/10.1127/njgpa/215/2000/69

Langer, M.C., Abdala, F., Richter, M. & Benton, M.J. 1999. A sauropodomorph dinosaur from the Upper Triassic (Carnian) of southern Brazil. *Comptes Rendus de l'Académie des Sciences - Series IIA - Earth and Planetary Science*, 329(7): 511-517. https://doi.org/10.1016/S1251-8050(00)80025-7

Langer, M.C., Eltink, E., Bittencour, J.S. & Rohn, R. 2009. Serra do Cadeado, PR - Uma janela paleobiológica para o Permiano continental sul-americano (Sítio 007). In: Winge, M., Schobbenhaus, C., Souza, C.R.G., Fernandes, A.C.S., Berbert-Born, M., Queiroz, E.T. & Campos, D.A. (Eds.). *Sítios Geológicos e Paleontológicos do Brasil*, v. II, Brasília, p. 433-450.

Langer, M.C., Ramezani, J. & Da Rosa, A. 2018. U-Pb age constraints on dinosaur rise from South America. *Gondwana Research*, 57: 133-140. https://doi.org/10.1016/j. gr.2018.01.005

Lavina, E.L. 1991. *Geologia sedimentar e paleogeografia do Neopermiano e Eotriássico (intervalo Kazaniano-Scithiano) da Bacia do Paraná*. Porto Alegre, 333p. Tese de Doutorado, Programa de Pós-graduação em Geociências, Instituto de Geociências, Universidade Federal do Rio Grande do Sul.

Lukens, W.E., Grandstalf, D.E. & Terry Jr., D.O. 2009. Rare earth element signatures in fossil bones: a tool for mitigating fossil poaching on federal lands. In: *PROCEEDINGS OF THE EIGHT CONFERENCE ON FOSSIL RESOURCES*, v. 8, p. 10-13.

Macfadden, B.J., Purdy, B.A., Church, K. & Stafford, T.W. 2012. Humans were contemporaneous with late Pleistocene mammals in Florida: evidence from rare earth elemental analyses. *Journal of Vertebrate Paleontology*, 32(3): 708-716. https://doi.org/10.1080/02724634.2012.655639

Malabarba, M.C., Abdala, F., Weiss, F. & Perez, P.A. 2003. New data on the Permian fauna of Posto Queimado, Rio do Rasto Formation, southern Brazil. *Revista Brasileira de Paleontologia*, 6: 49-54.

Martill, D. 1988. Preservation of fish in the Cretaceous Santana Formation of Brazil. *Palaeontology*, 31(1): 1-18.

Martin, E.E. & Scher, H.D. 2004. Preservation of seawater Sr and Nd isotopes in fossil fish teeth: bad and good news. *Earth and Planetary Science Letters*, 220(1–2,): 25-39. https://doi.org/10.1016/S0012-821X(04)00030-5

Martin, J.E., Patrick, D., Kihm, A.J., Foit, Jr., F.F., & Grandstaff, D.E. 2005. Lithostratigraphy, tephrochronology, and rare earth element geochemistry of fossils at the classical Pleistocene Fossil Lake Area, south central Oregon. *Journal of Geology*, 113(2): 139-155. https://doi.org/10.1086/427665

Martinelli, A.G., Bonaparte, J.F., Schultz, C.L. & Rubert, R. 2005. A new tritheledontid (Therapsida, Eucynodontia) from the Late Triassic of Rio Grande do Sul (Brazil) and its phylogenetic relationships among carnivorous non-mammalian eucynodonts. *Ameghiniana*, 42(1): 191-208. https://www.ameghiniana.org.ar/index.php/ameghiniana/article/view/882

Martinelli, A.G., Soares, M.B. & Schwanke, C. 2016. Two new cynodonts (Therapsida) from the Middle-Early Late Triassic of Brazil and comments on South American Probainognathians. *PloS One*, 11(10): e0162945. https://doi.org/10.1371/journal.pone.0162945

Martinelli, A.G., Kammerer, C.F., Melo, T.P., Paes Neto, V.D., Ribeiro, A.M., Da-Rosa, Á.A.S., Schultz, C.L. & Soares, M.B. 2017. The African cynodont Aleodon (Cynodontia, Probainognathia) in the Triassic of southern Brazil and its biostratigraphic significance. *PLoS One*, 12(6): e0177948. https://doi.org/10.1371/journal.pone.0177948

Melo, T.P., Abdala, F. & Soares, M.B. 2015. The Malagasy cynodont Menadon besairiei (Cynodontia; Traversodontidae) in the Middle–Upper Triassic of Brazil. *Journal of Vertebrate Paleontology*, 35(6): e1002562. https://doi.org/10.1080/02724634.2014.1002562

Metzger, C., Terry Jr., D.O. & Grandstaff, D.E. 2004. Effects of paleosol formation on rare earth element signatures in fossil bone. *Geology*, 32(6): 497-500. https://doi.org/10.1130/G20376.1

Milani, E.J., Faccini, U.F., Scherer, C.M.S., Araújo, L.M. & Cupertino, J.A. 1998. Sequences and stratigraphic hierarchy of the Paraná Basin (Ordovician to Cretaceous), Southern Brazil. *Boletim do Instituto de Geociências USP*, 29: 125-173.

Milani, E.J., Melo, J.H.G., Souza, P.A., Fernandes, L.A. & França, A.B. 2007. Bacia do Paraná. *Boletim de Geociências da Petrobras*, 15(2): 265-287.

Müller, R.T., Langer, M.C. & Dias-da-Silva, S. 2018. An exceptionally preserved association of complete dinosaur skeletons reveals the oldest long-necked sauropodomorphs. *Biology Letters*, 14: 20180633. https://doi.org/10.1098/rsbl.2018.0633

Müller, R.T., Ezcurra, M.D., Garcia, M.G., Agnolín, F.L., Stocker, M.R., Novas, F.E., Soares, M.B., Kellner, A.W.A. & Nesbitt, S.J. 2023. New reptile shows dinosaurs and pterosaurs evolved among diverse precursors. *Nature*, (7974): 589-594. https://doi.org/10.1038/s41586-023-06359-z

Neregato, R. 2007. *Estudo palinológico das formações Serra Alta, Teresina e Rio do Rasto nos furos de sondagem SP-23-PR e SP-58-PR, centro norte do Paraná (Permiano, Bacia do Paraná)*. 107p., M.Sc. thesis. Programa de Pós-Graduação em Geologia Regional, Instituto de Geociências e Ciências Exatas, UNESP.

Neregato, R., Souza, P.A. & Rohn, R. 2008. Registros palinológicos inéditos nas formações Teresina e Rio do Rasto (Permiano, Grupo Passa Dois, Bacia do Paraná): implicações biocronoestratigráficas e paleoambientais. *Pesquisas em Geociências*, 35(2): 9-21. https://doi.org/10.22456/1807-9806.17933

Nesbitt, H.W. 1979. Mobility and fractionation of rare earth elements during weathering of a granodiorite. *Nature*, 279: 206-210. https://doi.org/10.1038/279206a0

Newesely, H. 1989. Fossil bone apatite. *Applied Geochemistry*, 4(3): 233-245. https://doi.org/10.1016/0883-2927(89)90023-1

Ng, C., Vega, C.S. & Maranhão, M.S.A.S. 2019. Mixed carbonate-siliciclastic microfacies from Permian deposits of Western Gondwana: evidence of gradual marine to continental transition or episodes of marine transgression? Sedimentary Geology, 390: 62-82. https://doi.org/10.1016/j.sedgeo.2019.07.006

Nothdurft, L.D., Webb, G.E. & Kamber, B.S. 2004. Rare earth element geochemistry of Late Devonian reefal carbonates, Canning Basin, Western Australia: confirmation of a seawater REE proxy in ancient limestones. Geochimica et Cosmochimica Acta, 68(2): 263-283. https://doi.org/10.1016/S0016-7037(03)00422-8

Nozaki, Y., Zhang, J. & Amakawa, H. 1997. The fractionation between Y and Ho in the marine environment. *Earth and Planetary Science Letters*, 148(1–2): 329-340. https://doi.org/10.1016/S0012-821X(97)00034-4

Nozaki, Y., Lerche, D., Alibo, D.S. & Snidvongs, A. 2000. The estuarine geochemistry of rare earth elements and indium in the Chao Phraya River, Thailand. *Geochimica et Cosmochimica Acta*, 64(23): 3983-3994. https://doi.org/10.1016/S0016-7037(00)00473-7

Oelofsen, B. & Araújo, D.C. 1983. Paleoecological implications of the distribution of Mesosaurid reptiles in the Permian Irati sea (Paraná Basin), South America. São Paulo. *Revista Brasileira de Geociências*, 13(1): 1-16. https://doi.org/10.25249/0375-7536.19831310106

Oliveira, T.V., Soares, M.B. & Schultz, C.L. 2010. Trucidocynodon riograndensis gen. nov. et sp. nov. (Eucynodontia), a new cynodont from the Brazilian Upper Triassic (Santa Maria Formation). *Zootaxa*, 2382(1): 1-71. https://doi.org/10.11646/zootaxa.2382.1.1

Paes-Neto, V.D., Lacerda, M.B., Ezcurra, M.D., Raugust, T., Trotteyn, M.J., Soares, M.B., Schultz, C.L., Pretto, F.A., Francischini, H. & Martinelli, A.G. 2024. New rhadinosuchine proterochampsids from the late Middle-early Late Triassic of southern Brazil enhance the diversity of archosauriforms. *The Anatomical Record*, 307(4): 851-889. https://doi.org/10.1002/ar.25294

Pasteris, J.D., Wopenka, B. & Valsami-Jones, E. 2008. Bone and tooth mineralization: why apatite?. *Elements*, 4(2): 97-104. https://doi.org/10.2113/GSELEMENTS.4.2.97

Patrick, D., Martin, J.E., Parris, D.C. & Grandstaff, D.E. 2004. Paleoenvironmental interpretations of rare earth element signatures in mosasaurus (Reptilia) from the Upper Cretaceous Pierre Shale, central South Dakota, USA. Palaeogeography, Palaeoclimatology, Palaeoecology, 212(3–4): 277-294. https://doi.org/10.1016/j.palaeo.2004.06.005

Pauliv, V.E., Martinelli, A.G., Francischini, H., Dentzien-Dias, P., Soares, M.B., Schultz, C.L. & Ribeiro, A.M. 2017. The first western gondwanan species of Triodus Jordan 1849: a new xenacanthiformes (chondrichthyes) from the late paleozoic of southern Brazil. *Journal of South American Earth Sciences*, 80: 482-493. https://doi.org/10.1016/j.jsames.2017.09.007

Pearson, R.G. 1963 Hard and soft acids and bases. *Journal of the American Chemical Society*, 85(22): 3533-3539. https://doi.org/10.1021/ja00905a001

Philipp, R.P., Schultz, C.L., Kloss, H.P., Horn, B.L.D., Soares, M.B. & Basei, M.A.S. 2018. Middle Triassic SW Gondwana paleogeography and sedimentary dispersal revealed by integration of stratigraphy and U-Pb zircon analysis: the Santa Cruz Sequence, Paraná Basin, Brazil. *Journal of South American Earth Sciences*, 88: 216-237. https://doi.org/10.1016/j. jsames.2018.08.018

Philipp, R.P., Faccini, U.F., Schultz, C.L., Zvirtes, G., Bruckmann, M.P., Lavina, E., Cagliari, J., Jelinek, A.R., Netto, R.G., Viana, A.R. & Basei, M.A.S. 2023. U-Pb Zircon Geochronology of Detrital and Ash Fall Deposits of the Southern Paraná Basin: A Contribution for Provenance, Tectonic Evolution, and the Paleogeography of the SW Gondwana. Geosciences, 13(8): 225. https://doi.org/10.3390/geosciences13080225

Price, L.I. 1947. Um procolofonídeo do Triássico do Rio Grande do Sul. *Boletim da Divisão de Geologia e Paleontologia*, 22: 7-27.

Purdy, A.A., Rohkwing, K.M. & Macfadden, B.J. 2015. Devil's Den, Florida: Rare Earth Element Analysis Indicates Contemporaneity of Humans and Latest Pleistocene Fauna. *PaleoAmerica*, 1(3): 266-275. ttps://doi.org/10.1179/2055556315Z.00000000032

Reichel, M., Schultz, C.L. & Pereira, V.P. 2005. Diagenetic pattern of the vertebrate fossils from the Traversodontid Biozone, Santa Maria Formation (middle Triassic of Rio Grande do Sul, southren Brazil). *Revista Brasileira de Paleontologia*, 8(3): 173-180. https://doi.org/10.4072/rbp.2005.3.01

Richter, M. & Langer, M.C. 1998. Fish remains from the upper Permian Rio do Rasto formation (Paraná Basin) of southern Brazil. *Journal of African Earth Sciences*, 27(1): 158-159.

Rodrigues, I.C., Mizusaki, A.M.P., Lima, L.G & Maraschin, A.J. 2019. Comparative evolution of clay minerals in southern Paraná Basin (Brazil): implications for Triassic paleoclimate. Journal of South American Earth Sciences, 90: 181-190. https://doi.org/10.1016/j.jsames.2018.12.012

Rohn, R. 1994. *Evolução ambiental da Bacia do Paraná durante o Neopermiano no leste de Santa Catarina e do Paraná*. 251p., Unpublished Ph.D. thesis, Universidade de São Paulo, São Paulo.

Rohn, R. & Rösler, O. 1990. Conchostráceos da Formação Rio do Rasto (Bacia do Paraná, Permiano Superior): Bioestratigrafia e implicações paleoambientais. *Revista Brasileira de Geociências*, 9(4): 486-493.

Rohn, R. & Rösler, O. 2000. Middle to Upper Permian Phytostratigraphy of the Eastern Paraná Basin. *Revista da Universidade de Guarulhos*, 5: 69-73.

Rohn, R., Assine, M.L. & Meglhioratti, T. 2005. *A new insight on the Late Permian environmental changes in the Paraná Basin, South Brazil*. Gondwana 12, Mendoza- Argentina, Academia Nacional de Ciências, 316 pp.

Santos, R.V., Souza, P.A., Alvarenga, C.J.S., Dantas, E.L., Pimentel, M.M., Oliveira, C.G. & Araújo, L.M. 2006. Shrimp U-Pb Zircon dating and palinology of bentonitic layers from the Permian Irati Formation, Paraná Basin, Brazil. *Gondwana Research*, 9(4): 456-463. https://doi.org/10.1016/j.gr.2005.12.001

Scartezini, C.A., Battista, F., Martinelli, A.G., Paes Neto, V.D., Schultz, C.L., Pinheiro, F.L., Soares, M.B. 2025. Refinement of the Brazilian Hyperodapedon Assemblage Zone (Late Triassic) and its biostratigraphic correlation with the Argentine biozones of the Ischigualasto Formation. *Journal of South American Earth Sciences*, 164: 105641. https://doi.org/10.1016/j.jsames.2025.105641

Schemiko, D.C.B., Vesely, F.F., Fernandes, L.A. & Sowek, G.A. 2014. Distinção dos elementos deposicionais fluviais, eólicos e lacustres do Membro Morro Pelado, Permiano Superior da Bacia do Paraná. *Geologia USP. Série Científica*, 14: 29-46. https://doi.org/10.5327/Z1519-874X201400030003

Scherer, C.M.S. & Faccini, U.F. 1994. Análise faciológica do topo da formação Santa Maria (Triássico Superior da Bacia do Paraná) na região de Candelária-RS. In: *Anais...* 38° CONGRESSO BRASILEIRO DE GEOLOGIA, v.1, p. 85-86.

Scherer, C.M.S., Faccini, U.F., Barberena, M.C., Schultz, C.L. & Lavina, E.L. 1995. Bioestratigrafia da Formação Santa Maria: utilização das cenozonas como horizontes de correlação. Comunicações do Museu de Ciências e Tecnologia UBEA/PUCRS, *Série Ciências da Terra*, 1: 43-50.

Scherer, C.M.S., Reis, A.D., Horn, B.L.D., Bertolini, G., Lavina, E.L.C., Kifumbi, C. & Aguilar, C.G. 2023. The stratigraphic puzzle of the permo-mesozoic southwestern Gondwana: The Paraná Basin record in geotectonic and palaeoclimatic context. *Earth-Science Reviews*, 240: 104397. https://doi.org/10.1016/j.earscirev.2023.104397

Schmitt, M.R., Martinelli, A.G., Melo, T.P. & Soares, M.B. 2019. On the occurrence of the traversodontid *Massetognathus ochagaviae* (Synapsida, Cynodontia) in the early Late Triassic *Santacruzodon* Assemblage Zone (Santa Maria Supersequence, southern Brazil): Taxonomic and biostratigraphic implications. *Journal of South American Earth Sciences*, 93: 36-50. https://doi.org/10.1016/j.jsames.2019.04.011

Schneider, R.L., Mühlmann, H., Tommasi, E., Medeiros, R.A., Daemon, R.F. & Nogueira, A.A. 1974. Revisão estratigráfica da Bacia do Paraná. In: *Anais...* CONGRESSO BRASILEIRO DE GEOLOGIA, 28, 1974, Porto Alegre. Anais… Porto Alegre, SBG, v. 1, p. 41-65.

Schultz, C.L. 2005. Biostratigraphy of the Non-Marine Triassic: Is a global correlation based on tetrapod faunas possible? In: Koutsoukos, E.A.M. (Ed.). *Applied Stratigraphy*. Dordrecht, Springer, p.123-145. https://doi.org/10.1007/1-4020-2763-X_6

Schultz, C.L., Langer, M.C. & Montefeltro, F.C. 2016. A new rhynchosaur from south Brazil (Santa Maria Formation) and rhynchosaur diversity patterns across the Middle-Late Triassic boundary. *PalZ*, 90: 643-643. https://doi.org/10.1007/s12542-016-0307-7

Schultz, C.L., Martinelli, A.G., Soares, M.B., Pinheiro, F.L., Kerber, L., Horn, B.L.D., Pretto, F.A., Müller, R.T. and Melo, T.P. 2020. Triassic faunal successions of the Paraná Basin, southern Brazil. *Journal of South American Earth Sciences*, 104: 102846. https://doi.org/10.1016/j. jsames.2020.102846.

Shannon, R.D. 1976. Revised effective ionic radii and systematic studies of interatomic distances in halides and chalcogenides. *Acta Crystallographica Section A*, 32(5): 751-767. https://doi.org/10.1107/S0567739476001551

Silva Santos, O. 1998. Técnicas de Preparação de Fósseis. Departamento Nacional de Produção Mineral, Série Geologia nº 26, *Seção de Paleontologia e Estratigrafia*, 1: 101-127.

Simões, M.G., Rodrigues, S.C., Bertoni-Machado, C. & Holz, M. 2010. Tafonomia: Processos e ambientes de fossilização. In: Carvalho, I.S. (Ed.). *Paleontologia – Conceitos e Métodos*. 3ª ed., Rio de Janeiro, Ed. Interciência, v. 1, p. 19–51.

Simões, M.G., Matos, S.A., Anelli, L.E., Rohn, R., Warren, L.V. & David, J.M. 2015. A new Permian bivalve-dominated assemblage in the Rio do Rasto Formation, Paraná Basin, Brazil: faunal turnover driven by regional-scale environmental changes in a vast epeiric sea. *Journal of South American Earth Sciences*, 64: 14-26. https://doi.org/10.1016/j.jsames.2015.09.009

Slansky, M. 1980. *Géologie des phosphates sédimentaires*. Mém. BRGM, (114): 92p.

Soares, M.B. 2003. A taphonomic model for the mesosauride assemblage of the Irati Formation (Paraná Basin, Brazil). *Geologica Acta*, 1(4): 349-361. https://doi.org/10.1344/105.000001621

Soares, M.B., Schultz, C.L. & Horn, B.L.D. 2011. New information on Riograndia guaibensis Bonaparte, Ferigolo & Ribeiro, 2001 (Eucynodontia, Tritheledontidae) from the Late Triassic of southern Brazil: anatomical and biostratigraphic implications. *Anais da Academia Brasileira de Ciências*, 83(1): 329-354. https://doi.org/10.1590/S0001-37652011000100021

Staron, R.M., Grandstaff, B., Gallacher, W. & Grandstaff, D.E. 2001. REE Signatures in Vertebrate Fossils from Sewell, NJ: implications for Location of the K-T Boundary. *Palaios*, 16(3): 255-265. https://doi.org/10.2307/3515603

Suarez, C.A. 2004. Taphonomy and Rare Earth Element Geochemistry of the Stegosaurus sp. at the Cleveland Lloyd Dinosaur Quarry. In*: NORTHEASTERN SECTION (39TH ANNUAL) AND SOUTHEASTERN SECTION (53RD ANNUAL) JOINT MEETING (MARCH 25-27, 2004)*, p. 97.

Suarez, C.A., Suarez, M.B., Terry Jr., D.O. & Grandstaff, D.E. 2007. Rare earth element geochemistry and taphonomy of the Early Cretaceous Crystal Geyser Dinosaur Quarry, east-central Utah. Palaios, 22(5): 500-512. https://doi.org/10.2110/palo.2005.p05-126r

Suarez, C.A., Macpherson, G.L. & Grandstaff, D.E. 2009. Rare earth element geochemistry of fossil bone: using geochemical patterns to trace illegally excavated fossils. In: *PROCEEDINGS OF THE EIGHT CONFERENCE ON FOSSIL RESOURCES*, p. 19-21.

Suarez, C.A., Macpherson, G.L., Gonzalez, L.A. & Grandstaff, D.E. 2010. Heterogeneous rare earth element (REE) patterns and concentrations in a fossil bone: implications for the use of REE in vertebrate taphonomy and fossilization history. *Geochimica et Cosmochimica Acta*, 74(10): 2970-2988. https://doi.org/10.1016/j.gca.2010.02.023

Taylor, S.R. & McLennan, S.M. 1985. *The Continental Crust: Its Composition and Evolution*. Oxford, Blackwell Scientific, 312p.

Terry Jr., D.O., Grandstaff, D.E., Lukens, W.E. & Beasley, B.A. 2009. The use of rare earth element signatures in vertebrate fossils as a tool to investigate fossil poaching: a cooperative effort between Nebraska Forest and Temple University. In: *PROCEEDINGS OF THE EIGHT CONFERENCE ON FOSSIL RESOURCES*, p. 19-21.

Toledo, M.C.M. & Pereira, V.P. 2001. A variabilidade de composição da apatita associada a carbonatitos. *Revista do Instituto Geológico*, 22(1/2): 27-64.

Trueman, C.N. 2008. Trace element geochemistry of bonebeds. In: Rogers, R.R., Eberth, D.A. & Fiorillo, A.R. (Eds.). *Bonebeds. Genesis, Analysis, and Paleobiological Significance*. Chicago and London, The University of Chicago Press, p. 397-436. https://doi.org/10.7208/chicago/9780226723730.003.0007

Trueman, C.N. & Tuross, N. 2002. Trace elements in recent and fossil bone apatite. In: Kohn, M.J., Rakovan, J. & Hughes, J.M. (Eds.). *Reviews in Mineralogy and Geochemistry*, 48(1), p. 489-521. https://doi.org/10.2138/rmg.2002.48.13

Trueman, C.N., Reid, J.H., Dortch, J., Charles, B. & Wroe, S., 2005. Prolonged coexistence of humans and megafauna in Pleistocene Australia. *PNAS*, 102(23): 8381-8385. https://doi.org/10.1073/pnas.0408975102

Trueman, C.N., Palmer, M.R., Field, J., Privat, K., Ludgate, N., Chavagnac, V., Eberth, D.A., Cifelli, R. & Rogers, R.R. 2008a. Comparing rates of recrystallisation and the potential for preservation of biomolecules from the distribution of trace elements in fossil bones. *Comptes Rendus Palevol*, 7(2–3): 145-158. https://doi.org/10.1016/j.crpv.2008.02.006

Trueman, C.N., Privat, K. & Field, J. 2008b. Why do crystallinity values fail to predict the extent of diagenetic alteration of bone mineral? *Palaeogeography, Palaeoclimatology, Palaeoecology*, 266(3–4): 160-167. https://doi.org/10.1016/j.palaeo.2008.03.038

Turner-Walker, G. & Syversen, U. 2002, Quantifying histological changes in archaeological bones using BSE–SEM image analysis. Archaeometry, 44(3): 461-468. https://doi.org/10.1111/1475-4754.t01-1-00078

Tütken, T., Vennemann, T.W. & Pfretzschner, H.-U. 2011. Nd and Sr isotope compositions in modern and fossil bones—proxies for vertebrate provenance and taphonomy. *Geochimica et Cosmochimica Acta*, 75(20): 5951-5970. https://doi.org/10.1016/j.gca.2011.07.024

Valley, J.W., Essene, E.J. & Peacor, D.R. 1983. Fluorine-bearing garnets in Adirondack calc-silicates. *American Mineralogist*, 68(3–4): 444-448.

Williams-Jones, A.E., Migdisov, A.A. & Samson, I.M. 2012. Hydrothermal mobilisation of the rare earth elements–a tale of “ceria” and “yttria”. *Elements*, 8(5): 355-360. https://doi.org/10.2113/gselements.8.5.355

Wopenka, B. & Pasteris, J.D. 2005. A mineralogical perspective on the apatite in bone. *Materials Science and Engineering: C*, 25(2): 131-143. https://doi.org/10.1016/j.msec.2005.01.008

Wright, J., Schrader, H. & Holser, W.T. 1987. Paleoredox variations in ancient oceans recorded by rare earth elements in fossil apatite. *Geochimica et Cosmochimica Acta*, 51(3): 631-644. https://doi.org/10.1016/0016-7037(87)90075-5

Xavier, P.A., Silva, A.F., Soares, M.B., Horn, B.L.D. & Schultz, C.L. 2018. Sequence stratigraphy control on fossil occurrence and concentration in the epeiric mixed carbonate-siliciclastic ramp of the Early Permian Irati Formation of southern Brazil. *Journal of South American Earth Sciences*, 88: 157-178. https://doi.org/10.1016/j.jsames.2018.08.014

Zabini, C., Basso, J.M.L. & Martine, A.M. 2017. *Fossildiagênese. In: Horodyski, R.S. & Erthal, F. (Eds.). Tafonomia - Métodos, processos e aplicação*. Curitiba, Editora CRV, p. 343-368.

Zerfass, H., Lavina, E.L., Schultz, C.L., Garcia, A.G.V., Faccini, U.F. & Chemale Jr., F. 2003. Sequence stratigraphy of continental Triassic strata of southernmost Brazil: a contribution to Southwestern Gondwana palaeogeography and palaeoclimate. *Sedimentary Geology*, 161(1–2): 85-105. https://doi.org/10.1016/S0037-0738(02)00397-4

Zhang, K. & Shields, G.A. 2022. Sedimentary Ce anomalies: Secular change and implications for paleoenvironmental Evolution. Earth-Science Reviews, 229: 1-31. https://doi.org/10.1016/j.earscirev.2022.104015